Inorganic Chemistry

Article

pubs.acs.org/IC

Effect of N^4-Substituent Choice on Spin Crossover in Dinuclear Iron(II) Complexes of Bis-Terdentate 1,2,4-Triazole-Based Ligands

Jonathan A. Kitchen,[†] Juan Olguín,[†] Rafal Kulmaczewski,[†] Nicholas G. White,[†] Victoria A. Milway,[†] Guy N. L. Jameson,[†] Jeffery L. Tallon,[‡] and Sally Brooker*[,†]

[†]Department of Chemistry and the MacDiarmid Institute for Advanced Materials and Nanotechnology, University of Otago, P.O. Box 56, Dunedin 9054, New Zealand

[‡]MacDiarmid Institute for Advanced Materials and Nanotechnology, Callaghan Innovation, P.O. Box 31310, Lower Hutt 5040, New Zealand

Supporting Information

ABSTRACT: Seven new dinuclear iron(II) complexes of the general formula $[Fe^{II}_2(\mathbf{PMRT})_2](BF_4)_4$·solvent, where **PMRT** is a 4-substituted-3,5-bis{[(2-pyridylmethyl)-amino]methyl}-4*H*-1,2,4-triazole, have been prepared in order to investigate the substituent effect on the spin crossover event. Variable temperature magnetic susceptibility and ^{57}Fe Mössbauer spectroscopy studies show that two of the complexes, $[Fe^{II}_2(\mathbf{PMPT})_2](BF_4)_4$·$H_2O$ (N^4 substituent is pyrrolyl) and $[Fe^{II}_2(\mathbf{PM^{Ph}AT})_2](BF_4)_4$ (N^4 is *N*,*N*-diphenylamine), are stabilized in the [HS−HS] state between 300 and 2 K with weak antiferromagnetic interactions between the iron(II) centers. Five of the complexes showed gradual half spin crossover, from [HS−HS] to [HS−LS], with the following $T_{1/2}$ (K) values: 234 for $[Fe^{II}_2(\mathbf{PMibT})_2](BF_4)_4$·$3H_2O$ (N^4 is isobutyl), 147 for $[Fe^{II}_2(\mathbf{PMBzT})_2](BF_4)_4$ (N^4 is benzyl), 133 for $[Fe^{II}_2(\mathbf{PM^{CF3}PhT})_2](BF_4)_4$·DMF·$H_2O$ (N^4 is 3,5-bis(trifluoromethyl)phenyl), 187 for $[Fe^{II}_2(\mathbf{PMPhT})_2](BF_4)_4$ (N^4 is phenyl), and 224 for $[Fe^{II}_2(\mathbf{PMC_{16}T})_2](BF_4)_4$ (N^4 is hexadecyl). Structure determinations carried out for three complexes, $[Fe^{II}_2(\mathbf{PMPT})_2](BF_4)_4$·4DMF, $[Fe^{II}_2(\mathbf{PMBzT})_2](BF_4)_4$·$CH_3CN$, and $[Fe^{II}_2(\mathbf{PM^{Ph}AT})_2](BF_4)_4$·solvent, revealed that in all three complexes both iron(II) centers are stabilized in the high spin state at 90 K. A general and reliable 4-step route to **PMRT** ligands is also detailed.

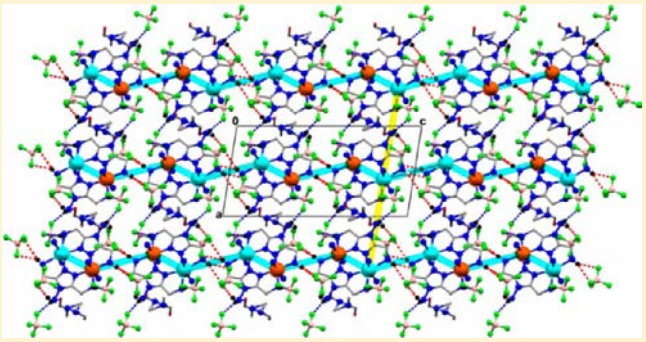

INTRODUCTION

The use of 1,2,4-triazole based ligands in combination with iron(II) is of significant interest because of the possibility of generating magnetically interesting complexes, specifically complexes that exhibit spin crossover (SCO). One of the avenues that we are investigating in this area is the preparation of discrete dinuclear iron(II) complexes that feature doubly bridging heterocyclic moieties. Dinuclear complexes allow the relationship between exchange coupling and SCO to be probed; they also lend themselves to the generation of complexes that might exhibit multiple SCO events. The latter property, preferably along with hysteresis (which is facilitated by communication between the metal ions), is desirable as such complexes might offer the longer term possibility of developing more dense information storage systems.[1−3]

While the development of dinuclear iron(II) complexes is becoming increasingly popular, there is currently a lack of control and predictability over the temperature at which an SCO event occurs.[3] A key exception to this generalization is the work of Kaizaki and co-workers on varying R in some doubly pyrazolate-bridged diiron(II) complexes of dipyridyl pyrazolate (bpypz) and substituted pyridines (Rpy), $[Fe^{II}_2(bpypz)_2(NCS)_2(Rpy)_2]$.[4] Inspired by this study, we embarked on attempts to investigate the features that influence SCO in iron(II) systems with the aim of gaining greater understanding and hence increased predictive powers. In particular, we have carried out systematic investigations aimed at testing whether or not further examples of correlations between ligand substitution patterns and the magnetic properties of the resulting complexes can be established.

1,2,4-Triazole rings are the ideal ligand scaffold for our purposes. Not only are triazoles well-documented to have a field strength in about the right range to induce SCO in iron(II), but also they have adjacent nitrogen atoms capable of bridging two metal centers. Furthermore, the N^4 position is available for substitution, facilitating the development of the family of subtly different ligands that we require. Finally, the C^3 and C^5 positions are also available for substitution so we have used these sites to incorporate further donor atoms, increasing the denticity of the ligand and generating two binding pockets bridged by N^1N^2 of the triazole moiety. In summary, the triazole ring is a highly versatile heterocycle for incorporation into ligands for complexation with iron(II) with the aim of preparing SCO active complexes.

Received: June 6, 2013
Published: September 20, 2013

   dx.doi.org/10.1021/ic4014416 | *Inorg. Chem.* 2013, 52, 11185−11199

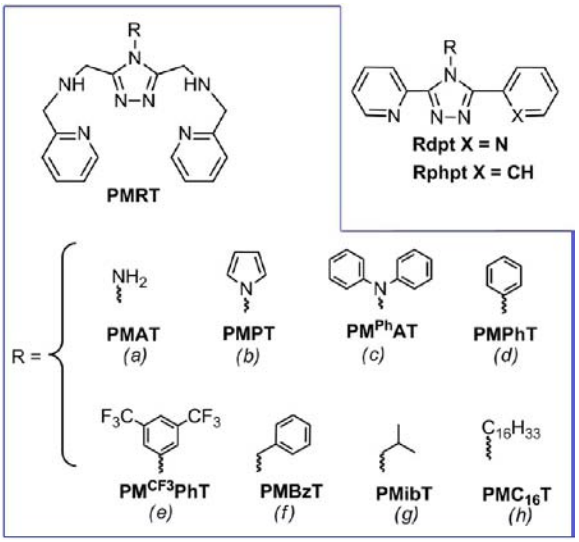

Figure 1. Triazole-based bis-terdentate **PMRT** ligands employed in this research (inside the box) and the related family of triazole-based bis-bidentate ligands **Rdpt**[5−11] and bidentate ligands **Rphpt**.[12]

Work utilizing such ligands with iron(II) has previously been carried out, by us and others, in particular with N^4-substituted-3,5-dipyridyl-1,2,4-triazole ligands (**Rdpt**).[5−13] We, and others, have used these potentially bis-bidentate **Rdpt** ligands to generate interesting mononuclear SCO active iron(II) complexes, $[Fe^{II}(\mathbf{Rdpt})_2(X)_2]$, X = NCE (E = S, Se, and BH_3), TCNQ, etc.[5,6,11,13] We have also reported a family of mostly low spin mononuclear $[Fe^{II}(\mathbf{Rdpt})_3](BF_4)_2$[10] complexes and of [HS−HS] dinuclear complexes $[Fe^{II}(\mathbf{Rdpt})_2(H_2O)_2(CH_3CN)_2](BF_4)_2$,[9] in which the R substituent on N^4 was systematically varied. However, when we attempted to prepare SCO-active dinuclear iron(II) complexes of these ligands (which the ligand design should allow for, by analogy with the dipyridylpyrazole ligands of Kaizaki and co-workers[4]) by introducing NCE coligands (E = S, Se, BH_3, etc), dinuclear complexes proved to be elusive.[9,10]

Hence, in order to more predictably generate dimetallic complexes, our focus reverted to triazole-based ligands of greater denticity, including those which offer bis-terdentate binding pockets. The unique SCO properties of the first example of such a dinuclear complex, $[Fe^{II}_2(\mathbf{PMAT})_2](BF_4)_4$·DMF (**PMAT** is N^4-amino-3,5-bis{[(2-pyridylmethyl)amino]methyl}-4*H*-1,2,4-triazole, Figure 1),[14−16] prompted us to prepare a family of related complexes in which the N^4-substituent R on the triazole ring (R = NH_2 in **PMAT**) is systematically altered, i.e., to prepare a new family of bis-terdentate **PMRT** ligands varying only in R (Figure 1) and use them to generate a family of SCO-active dinuclear complexes.

The primary goals for this research were therefore to (a) develop a general and reliable route to a family of N^4-substituted-3,5-bis[(2-pyridylmethyl)amino]methyl}-4*H*-1,2,4-triazole (**PMRT**) ligands (Figure 1) and (b) prepare and characterize dinuclear iron(II) complexes of the resulting family of **PMRT** ligands and investigate the effect of the N^4-substituent on the SCO behavior. Such studies are of considerable current interest to researchers in the SCO field as it is important to try to open up the possibilities of predicting which substituents will perturb

Scheme 1. Two Synthetic Routes to the PMRT Ligands[a]

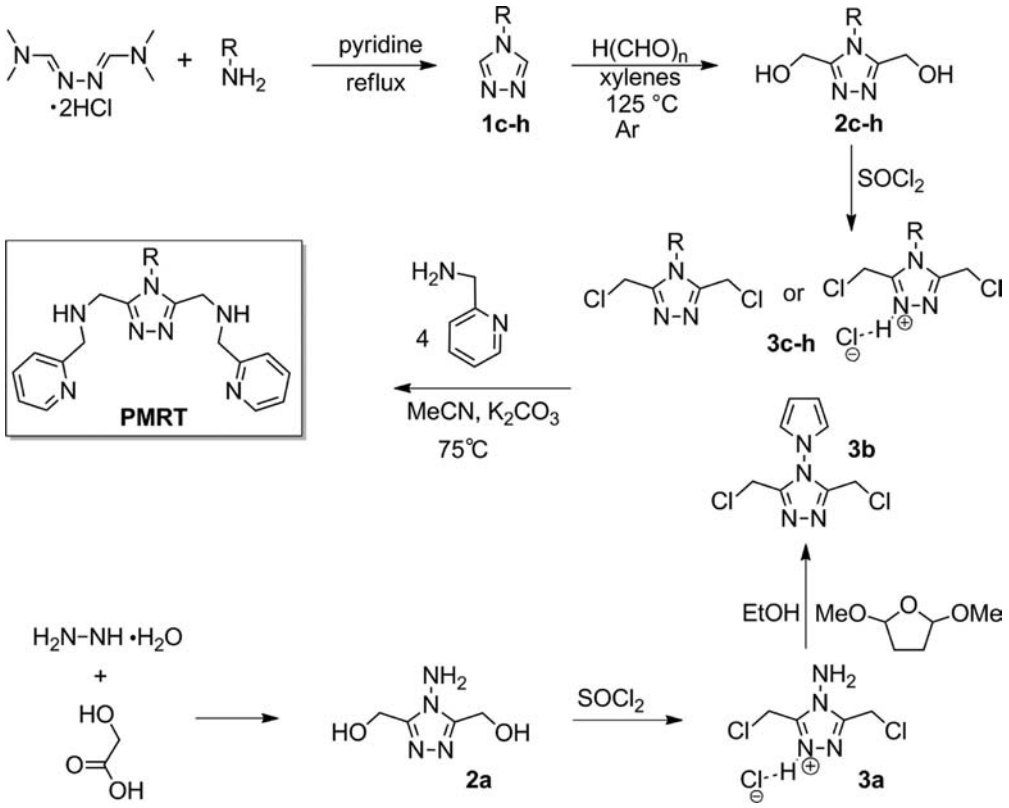

[a]R substituents are given in Figure 1. The top route is general and was used to generate **PMRT** ligands in which the R substituent link is either a C−N^4(triazole) or a N−N^4(triazole) bond (**PM^{Ph}AT**), whereas the bottom route results only in the link being an N−N^4(triazole) bond.

dx.doi.org/10.1021/ic4014416 | *Inorg. Chem.* 2013, 52, 11185−11199

the system sufficiently to induce SCO, and of predictably tuning $T_{1/2}$ by careful ligand design. Here we report our investigations into the effect of the N^4-substituent on the magnetic properties of the dinuclear iron(II) complexes of these bis-terdentate triazole based **PMRT** ligands.

RESULTS AND DISCUSSION

Synthesis of Ligands. The general and reliable route to **PMRT** ligands that we have developed and report herein comprises four steps (Scheme 1, top), the first of which is the formation of the triazole ring (**1c−h**) *via* transamination of *N,N*-dimethylformamide azine (prepared by the well established method[17]) with the chosen primary amine. The reaction protocol chosen was an adaptation of that reported by Bartlett and Humphrey in 1967,[17] where rather than using the free base azine in a stoichiometric ratio, the dihydrochloride salt was used in a slight excess (1.5 equiv) over the amine (1 equiv), and the reaction was carried out in refluxing pyridine, as reported by Robins and co-workers in the 1990s.[18] Using this method we have prepared six N^4-substituted-1,2,4-triazoles (Figure 1) in moderate to good yields (44−82%). It should be noted that five of these, **1c**, **1d**, **1f−h**, are literature compounds;[17,19] however, they were synthesized using slight variations on these methods.

The second, and key, step in our reaction protocol involves the hydroxymethylation of the C^3 and C^5 positions of the triazole rings of **1c−h** to form N^4-substituted-3,5-bis-(hydroxymethyl)-1,2,4-triazoles **2c−h**. The method used was similar to those reported by Hester for the hydroxymethylation of highly substituted triazoles[20] and Ivanova for the synthesis of 4,5-disubstituted 1,2,4-triazoles functionalized in position 3.[21] Triazoles **1c−h** (Scheme 1) were heated to 115 °C in xylenes under argon, and 10 equiv of paraformaldehyde was added. Once the entire portion of paraformaldehyde was added the temperature was raised to 125 °C and heating and stirring was continued under argon until the resulting suspension had become a clear solution. On observing this change a second portion (10 equiv) of paraformaldehyde was added, and heating continued. When reaction of the second portion of paraformaldehyde (**2e** was an exception to this and required addition of two further portions, see below) was completed (typically 6−8 h of total heating), the resulting reaction mixture was worked up. The workup of the hot reaction mixture varied because the nature of the precipitate differed in each case, as a function of the N^4-substituent. The major "contaminant" in most cases was the monohydroxymethylated species; however, solubility differences between this and the desired bis-hydroxymethylated species (bis is less soluble than mono) were sufficient to achieve separation. For example, some compounds only required filtering of the cooled reaction solution to afford the desired product (**2c**, **2d**, and **2g**); however, when the monohydroxymethylated species was also insoluble in cooled xylenes a diffferent approach was needed. In these cases, hot filtrations, at ∼80−100 °C, were carried out, as at higher temperatures the monohydroxymethylated compounds were soluble whereas the desired bis-hydroxymethylated compounds remained insoluble (**2e**, **2h**). In the case of **2f**, cooling the reaction gave a yellow waxy solid. Decanting off the xylenes and recrystallizing the waxy solid from hot water gave the desired compound as a white crystalline solid. The hydroxymethylation reactions gave moderate to good yields (46−77%) of the desired N^4-substituted-3,5-bis(hydroxymethyl)-1,2,4-triazoles (**2c−h**).

In just one case, the preparation of N^4-(3,5-bis(trifluoromethyl)-phenyl)-3,5-bis(hydroxymethyl)-1,2,4-triazole (**2e**), a total of 4 x 10 equiv of paraformaldehyde had to be added for a satisfactory yield to be obtained (55%), presumably because of the electron withdrawing nature of the N^4-substituent. Hydroxymethylation is an electrophilic process so it is unsurprising that electron donating/withdrawing groups will greatly affect the reaction, the latter adversely.

The third step in the synthesis of the **PMRT** ligands is the chlorination of the hydroxyl groups using thionyl chloride. Following the same procedure as in our published synthesis of **PMAT**,[14] chlorination of **2c−h** was achieved, resulting in a family of N^4-substituted-3,5-bis-chloromethyl-1,2,4-triazole hydrochlorides **3c−h** (Scheme 1). Specifically, addition of excess $SOCl_2$ to solids **2c−h** gave an exothermic reaction and resulted in a yellow solution that was stirred, while open to the air in a fume hood, overnight. This allowed evaporation of the excess $SOCl_2$, eliminating the need to remove it under reduced pressure the next day. Typically this resulted in pale white/yellow powders (**3c**, **3d**, **3g**, and **3h**) or sticky colorless oils (**3e**, **3f**). Drying the crude mixture *in vacuo* followed by recrystallization from absolute alcohol yields **3c−h** as colorless crystalline solids. All but **3c** and **3e** analyzed as mono hydrochloride salts; **3c** and **3e** analyzed as a mixture of $^1/_3$ neutral triazole species and $^2/_3$ hydrochloride salt. Crystal structure determinations were carried out for four of the seven hydrochloride salts, **3d** and **3f−h**. These confirmed the protonation of the triazole ring (charge balance provided by a chloride ion, i.e., +HCl overall) and allowed an initial analysis of how altering the N^4-substituent changes the crystal packing (see later; for full details see Supporting Information).

The reactions shown in Scheme 1 appear to be general for any N^4-substituent, and therefore, this approach should provide ready access to a huge variety of new N^4-substituted-3,5-bis-chloromethyl-1,2,4-triazole hydrochlorides (**3c−h**), from simple, commercially available, starting materials and on large scales. This opens up access to a wide range of new 3,5-disubstituted triazole ligands, with choice of N^4-substituent.

One of the desired dichloromethyl compounds, N^4-pyrrolyl-3,5-bis-chloromethyl-1,2,4-triazole (**3b**), was not prepared according to the above general synthesis but *via* the literature method.[14] While it is most likely possible to do so, we instead prepared it from N^4-amino-3,5-bis-chloromethyl-1,2,4-triazole hydrochloride (**3a**) as large amounts of **3a** were available due to our work with **PMAT**. Reaction of **3a** with 2,5-dimethoxytetrahydrofuran yielded the desired N^4-pyrrolyl dichloromethyl compound, **3b** (bottom route in Scheme 1).

The final step in the synthesis of all eight of the **PMRT** ligands presented in Scheme 1 is reaction of **3** with an excess of 2-aminomethylpyridine (4 equiv) and K_2CO_3 (6 equiv) in acetonitrile at 75 °C. After 7 h of heating with stirring, the reaction mixture was filtered through Celite, and all volatiles were removed from the filtrate under reduced pressure. The resulting brown residues were taken up in a methanol/ethanol (1:5) mixture and filtered through a short pad of neutral alumina to yield the desired **PMRT** ligands, contaminated with varying amounts of 2-aminomethylpyridine, as orange oils. These oils could be used in iron(II) complexation reactions, without any further purification, to generate analytically pure $[Fe^{II}_2(\mathbf{PMRT})_2](BF_4)_4 \cdot$ solvent complexes (see below).

Selection of Ligands. In a similar vein to our systematic investigation into a family of iron(II) tris-**Rdpt** systems,[10] the present N^4-substituted-3,5-bis{[(2-pyridylmethyl)amino]-methyl}-4*H*-1,2,4-triazole (**PMRT**) ligands also contain a variety

dx.doi.org/10.1021/ic4014416 | *Inorg. Chem.* 2013, 52, 11185−11199

of R substituents attached to the triazole N^4 position either through a nitrogen (**PMPT** and **PM^{Ph}AT**, Figure 1) or a carbon atom (**PMPhT**, **PM^{CF3}PhT**, **PMBzT**, **PMibT**, and **PMC$_{16}$T**, Figure 1).

The ligands with N^4-substituents attached through a nitrogen atom follow on from our work with the ligand **PMAT** (Figure 1). The inclusion of the pyrrolyl ring (**PMPT**) was made for the reasons discussed in our previous work;[10] i.e., it offers minimal π electron donation into the attached triazole ring due to being approximately at right angles to it. The diphenyl amino group adds a relatively large bulky group to the ligand (**PM^{Ph}AT**) so it may considerably alter the crystal packing interactions when compared to **PMAT** which has a much less bulky NH_2 group. The incorporation of carbon attached N^4-substituents allows for greater choice with respect to the nature of the substituent and the properties it imparts on the ligand. The **PMRT** ligands with an aromatic or substituted-aromatic substituent, phenyl (**PMPhT**) and 3,5-bis-trifluoromethyl-phenyl (**PM^{CF3}PhT**) N^4-substituents, were prepared as these should result in differences not only in the electronic properties, but also in the crystal packing as seen in the tris-**Rdpt** iron(II) series.[10] The inclusion of the benzyl group (**PMBzT**) gives an N^4-substituent that has a large bulky aromatic group yet is attached to the triazole through a CH_2 moiety which breaks the conjugation. Finally, two alkyl N^4-substituents were also examined, iso-butyl (**PMibT**) and hexadecyl (**PMC$_{16}$T**), the latter because of our interest in forming Langmuir–Blodgett films.[11,22]

Structures of the N^4-Substituted-3,5-bis(chloromethyl)-1,2,4-triazoles. X-ray quality single crystals of **3d** and **3f–h** were readily obtained from the slow evaporation of absolute ethanol solutions. Information pertaining to the relationship between N^4-substituent and crystal packing interactions is therefore readily acquired. Of particular interest is the orientation of the N^4-substituent R with respect to the attached triazole ring as this is likely to be crucial to extent of the impact R has on the N^1 and N^2 triazole donor atoms. Additionally, the intermolecular interactions that link neighboring molecules were investigated as these are likely to be important in communication between any subsequently prepared iron(II) complexes featuring bis-terdentate **PMRT** ligands prepared from these bis-chloromethyl triazoles. Full descriptions of the four crystal structures are available in the Supporting Information (see Figures 2 and 3 and Supporting Information Figures S1–S9), including detailed analyses of the packing interactions, but some of the key findings are provided here.

When the N^4-substituents are phenyl (**3d**), or benzyl (**3f**), no interactions involving the N^4-substituents are observed. However, when the N^4-substituents were alkyl [iso-butyl (**3g**) and hexadecyl (**3h**)] packing interactions involving these N^4-substituents were observed. In **3g**, weak nonclassical C–H···Cl hydrogen bonds occur between the hydrogen atoms of the iBu substituent, forming sheets which are linked to identical antiparallel sheets through further C–H···Cl interactions (Figure 2; see Supporting Information for details). The C_{16} chain of **3h** led to the formation of interdigitated layers (Figure 3), similar to those of a lipid bilayer. This type of arrangement is encouraging as it is ideal for the formation of Langmuir–Blodgett films,[23] an area that is of considerable interest to us as we move toward functional materials.[11,22]

Synthesis of Complexes. All seven complexes were prepared by the reaction of crude **PMRT** with excess iron(II) tetrafluoroborate (2 equiv) in HPLC grade methanol at room

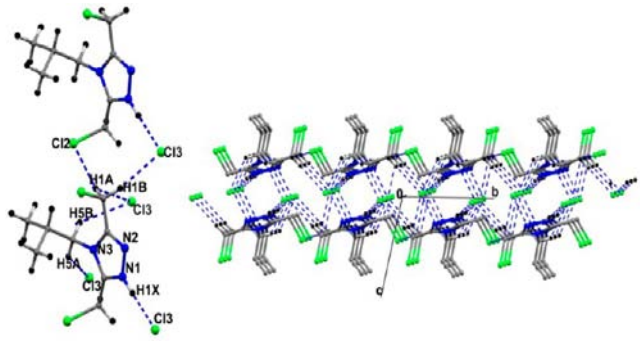

Figure 2. Left: Structure of **3g** highlighting H-bond interactions. Right: The antiparallel sheets of **3g** generated by these interactions.

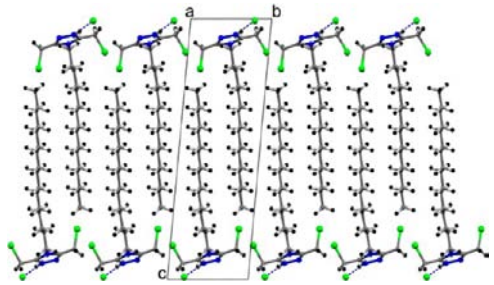

Figure 3. Bilayer formed by the interdigitating C_{16} chains in the structure of **3h**; view down the *a* axis.

temperature. The pale precipitate that formed was filtered and dried *in vacuo*, giving the desired complexes as analytically clean powders in reasonable yields (32–55%). These powders were crystallized from MeCN/DMF (4:1) by vapor diffusion of diethylether to give the crystalline or powder samples which were air-dried and used for magnetic measurements, namely $[Fe^{II}_2(\mathbf{PMPT})_2](BF_4)_4\cdot H_2O$, $[Fe^{II}_2(\mathbf{PM^{Ph}AT})_2](BF_4)_4$, $[Fe^{II}_2(\mathbf{PMPhT})_2](BF_4)_4$, $[Fe^{II}_2(\mathbf{PM^{CF3}PhT})_2](BF_4)_4\cdot DMF\cdot H_2O$, $[Fe^{II}_2(\mathbf{PMBzT})_2](BF_4)_4$, $[Fe^{II}_2(\mathbf{PMibT})_2](BF_4)_4\cdot 3H_2O$, and $[Fe^{II}_2(\mathbf{PMC_{16}T})_2](BF_4)_4$. The synthesis, recrystallization, and drying of these samples were deliberately carried out in the same solvents using the same protocols, due to the known sensitivity of SCO to solvent content and packing. The fact that, regardless of these efforts, a variety of solvent content is observed across this family of complexes is quite simply beyond our control, and is likely due to the wide variation of the size and nature of the R group.

In most cases it was not necessary to perform the reactions under an inert atmosphere; however, for the isobutyl and hexadecyl substituted ligands cleaner complexes were obtained when they were prepared and filtered under an argon atmosphere. The complexes were characterized by elemental analysis, mass spectrometry, infrared and Mössbauer spectroscopy, and variable temperature magnetic moment measurements. Where possible the complexes were also characterized by single crystal X-ray crystallography to confirm the overall structure of the complex and to allow a detailed packing analysis to be carried out.

Structures of the Dinuclear Iron(II) Complexes. SCO in iron(II) complexes can be very sensitive to the crystal morphology and solvent content. When a compound is obtained by slightly different methods, i.e., different solvents or isolation techniques, then the resulting magnetism can be dramatically altered.[3,6,7,24] For this reason we attempted to isolate and crystallize the complexes using the same method for all complexes.

dx.doi.org/10.1021/ic4014416 | *Inorg. Chem.* 2013, 52, 11185–11199

Table 1. Comparison of Selected Bond Distances (Å), Angles (deg), and Other Data for $[Fe^{II}_2(PM^{Ph}AT)_2](BF_4)_4$·solvent, $[Fe^{II}_2(PMPT)_2](BF_4)_4$·4DMF, $[Fe^{II}_2(PMBzT)_2](BF_4)_4$·$CH_3CN$, and the Previously Reported $[Fe^{II}_2(PMAT)_2](BF_4)_4$·DMF

				$[Fe_2(PMAT)_2](BF_4)_4$·DMF[15]	
selected parameters	$[Fe_2(PM^{Ph}AT)_2](BF_4)_4$·solvent 91 K [HS−HS]	$[Fe_2(PMPT)_2](BF_4)_4$·4DMF 90 K [HS−HS]	$[Fe_2(PMBzT)_2](BF_4)_4$·CH_3CN (89 K) [HS−HS]	123 K [HS−LS]	298 K [HS−HS]
Fe−N_{pyr} (Å)	Fe(1) 2.144(5), 2.128(5); Fe(2) 2.186(5), 2.159(5)	2.137(2), 2.125(2)	2.056(6), 2.058(6)	Fe(1) 1.987(4), 1.986(4); Fe(2) 2.155(4), 2.159(4)	2.147(5), 2.148(4)
Fe−N_{NH} (Å)	Fe(1) 2.291(4), 2.302(5); Fe(2) 2.270(5), 2.277(4)	2.334(2), 2.304(2)	2.159(7), 2.173(5)	Fe(1) 2.066(4), 2.071(4); Fe(2) 2.319(4), 2.312(4)	2.289(5), 2.303(5)
Fe−N_{triaz} (Å)	Fe(1) 2.123(5), 2.133(4); Fe(2) 2.135(4), 2.138(5)	2.102(2), 2.128(2)	2.020(4), 2.032(5)	Fe(1) 1.934(3), 1.946(3); Fe(2) 2.131(3), 2.136(3)	2.116(4), 2.123(4)
av Fe−N (Å)	Fe(1) 2.187; Fe(2) 2.194	2.188	2.083	Fe(1) 1.998; Fe(2) 2.202	2.188
cis-N−Fe−N range (deg)	Fe(1) 75.2(2) − 115.1(2); Fe(2) 76.1(2) − 116.0(2)	75.2(6)−114.9(6)	78.0(3)−111.0(2)	Fe(1) 81.8(1) −101.1(1); Fe(2) 75.1 (1) − 121.6(1)	75.92(2), 115.9(2)
trans-N−Fe−N range (deg)	Fe(1) 159.6(2)−167.3(2); Fe(2) 163.3(2)−165.3(2)	159.0(6)−169.3(6)	160.6(3)−171.1(2)	Fe(1) 171.0−(1)−175.9(2); Fe(2) 154.2 (1) − 163.2(1)	161.3(2), 167.7(2)
cis-N−Fe−N average (deg)	Fe(1) 90.6; Fe(2) 90.5	90.5	90.4	Fe(1) 90.07; Fe(2) 90.98	90.5
trans-N−Fe−N average (deg)	Fe(1) 164.3; Fe(2) 164.4	165.2	167.1	Fe(1) 174.1; Fe(2) 160.0	165.1
Σ (deg)[a]	Fe(1) 119.1; Fe(2) 116.1	119.9	99.4	Fe(1) 65.0; Fe(2) 133.1	117.5

[a]The octahedral distortion parameter, Σ, is defined as the sum of the absolute values of the difference of each of the 12 *cis* angles from 90°.

However, the only single crystals obtained were from attempts employing the diffusion of diethyl ether vapor into a solution of the complex in either pure DMF or acetonitrile:DMF mixture (4:1 v/v): this worked for three of the seven complexes, $[Fe^{II}_2(\mathbf{PMPT})_2](BF_4)_4$·4DMF, $[Fe^{II}_2(\mathbf{PM^{Ph}AT})_2](BF_4)_4$·solvent, and $[Fe^{II}_2(\mathbf{PMBzT})_2](BF_4)_4$·$CH_3CN$ (Table 1 and Supporting Information Table S2).

Crystals of $[Fe^{II}_2(\mathbf{PMPT})_2](BF_4)_4$·4DMF were obtained as pale yellow blocks by subjecting a DMF solution of the complex to diethyl ether vapor diffusion. At 90 K, the asymmetric unit contains one-half of the dinuclear complex, two anions, and two DMF solvent molecules, with the other half of the complex generated by a center of inversion between the two iron ions (Figure 4). The iron(II) center has a distorted

Figure 4. Perspective view of the structure of $[Fe^{II}_2(\mathbf{PMPT})_2](BF_4)_4$·4DMF. Color codes: iron, orange spheres; nitrogen, royal blue spheres; oxygen, red spheres; carbon, gray spheres; fluorine, green spheres; boron, tan spheres; and hydrogen, black spheres. H-bonds represented by blue dashed lines, anion−π interactions represented by green dashed lines, and light blue spheres marked 1 and 2 represent ring centroids.

octahedral N_6 coordination sphere (Table 1), comprising three nitrogen donor atoms from each of two **PMPT** ligands, which sandwich the two metal ions and provide all 12 donor atoms to them. The Fe−N bond lengths are long [2.102(2)−2.334(2) Å], and the *cis*-N−Fe−N angles range far from 90° [75.2(6)−114.9(6)°], consistent with the presence of HS iron(II) centers. A large twist is seen around the triazole-pyrrolyl N−N bond [75.4(1)°], as has previously been seen in N^4-pyrrolyl-1,2,4- triazole ligands and metal complexes.[25,26]

Hydrogen bonds[27] are observed between all four of the secondary amine protons and the BF_4 anions [blue dashed lines in Figure 4; N−H···F = 3.099(2)−3.115(2) Å, ∠(N−H···F) = 154−164°], as well as anion−π interactions[28] between the anions and the coordinated pyridine and triazole rings [green dashed lines in Figure 4; centroid 1···F22 = 3.197(2) Å and centroid 2···F23 = 3.120(2) Å]. For full details of all hydrogen-bonding and anion−π interactions, see Supporting Information Tables S3 and S4. Surprisingly short interactions are seen between the lone pair on the DMF oxygen atom and the

dx.doi.org/10.1021/ic4014416 | Inorg. Chem. 2013, 52, 11185−11199

triazole ring [centroid 1···O100 = 3.025(2) Å], with a longer interaction seen between the same DMF oxygen atom and a coordinated pyridine ring from the same complex [centroid 2···O100 = 3.197(2) Å]. Interestingly, this DMF solvate and one of the BF_4 anions sandwich the triazole ring (Figure 4), showing a similar electron pair···triazole···anion interaction to those observed in complexes of the related bis-bidentate ligand, **pldpt** (4-pyrrolyl-3,5-di(2-pyridyl)-1,2,4-triazole).[26,29]

$[Fe^{II}_2(\mathbf{PM^{Ph}AT})_2](BF_4)_4$·solvents crystallized from a 4:1 MeCN/DMF mixture, in the monoclinic space group $P2_1/c$ with one complete dinuclear complex and four tetrafluoroborate counteranions in the asymmetric unit (Figure 5; the solvent molecules were severely disordered and could not be sensibly refined, and so the SQUEEZE command in PLATON[30] was used to include this electron density in the refinement). Again the iron(II) centers are in a distorted N_6 coordination sphere where all 12 nitrogen atom donors are supplied by the two $\mathbf{PM^{Ph}AT}$ ligands (Table 1). The Fe−N bond lengths [2.123(5)−2.302(5) Å] and *cis*-N−Fe−N bond angles [75.2(2)−116.0(2)°] are consistent with those expected for HS iron(II). All four secondary amine protons make hydrogen bonds to fluorine atoms of the tetrafluoroborate counterions [blue dashed lines in Figure 5; N−H···F = 2.909(6)−3.166(5) Å and ∠(N−H···F) = 123−162°; see Supporting Information Table S5]. There is an anion−π interaction between F12 and the triazole ring of N3 [Figure 5; centroid 1···F12 = 3.229(7) Å; ∠(N3−centroid 1−F12) = 88.8(4)°; ∠(centroid 1−F12−B11) = 174.6(6)°]. The triazole ring of N43 also interacts with a tetrafluoroborate counteranion [centroid 2···F24 = 3.136(4) Å; centroid 2···F21 = 3.233(4) Å]. This time the counteranion sits almost directly above the triazole ring [∠(centroid 2−F21−B21) = 98.9(4)°; ∠(centroid 2−F24−B21) = 103.2(4)°] with the two interacting fluorine atoms F21 and F24 sitting directly above the triazole carbon atoms C48 and C49, respectively. Each of the triazole rings makes the anion−π interaction on one face, with the other face blocked by one of the two phenyl rings from the diphenylamino N^4-substituent. The pyridine ring of N1 is also involved in the π interactions with the tetrafluoroborate anions [centroid 3···F32 distance is 3.242(4) Å; ∠(centroid 3−F32−B31) = 119.3(4)°].

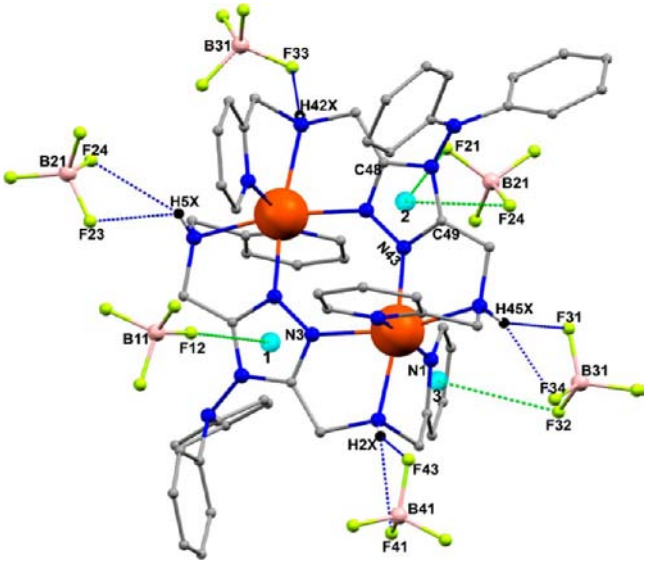

Figure 5. Perspective view of the structure of $[Fe^{II}_2(\mathbf{PMPhAT})_2](BF_4)_4$·solvents. Color codes: iron, orange spheres; nitrogen, royal blue spheres; oxygen, red spheres; carbon, gray spheres; fluorine, green spheres; boron, tan spheres; and hydrogen, black spheres. H-bonds represented by blue dashed lines, anion−π interactions represented by green dashed lines, and light blue spheres marked 1−3 represent ring centroids.

Crystals of $[Fe^{II}_2(\mathbf{PMBzT})_2](BF_4)_4$·$CH_3CN$ were obtained by slow diffusion of diethyl ether vapor into acetonitrile/DMF mixture (4:1 v/v). The complex crystallized in the monoclinic space group $P2_1/c$ with the asymmetric unit comprising half of the complex (the other half is generated by an inversion center between two iron ions), two tetrafluoroborate counteranions, and one full occupancy acetonitrile molecule (Figure 6). As in the **PMPT** and $\mathbf{PM^{Ph}AT}$ complexes, the crystallographically independent iron(II) center is coordinated by six nitrogen atoms from two **PMBzT** ligands with Fe−N distances [2.020(4)−2.173(5) Å] and *cis*-N−Fe−N angles [78.0(3)−111.0(2)°] typical for HS iron(II) centers (Table 1). Again, both secondary amine protons make hydrogen bonds to fluorine atoms of, in this case, the disordered, tetrafluoroborate anions [N−H···F = 3.023(8)−3.246(9) Å and ∠(N−H···F) = 128−159°; see Supporting Information Table S7]. The ordered BF_4 anion does not participate in the hydrogen bonding. The N3 triazole ring interacts with the lone pair of the nitrogen atom of an acetonitrile molecule [green dashed line in Figure 6; centroid 1···N100 distance = 3.183(7) Å; ∠(nitrile CN···centroid 1) = 162.6(6)°; see Supporting Information Table S8].

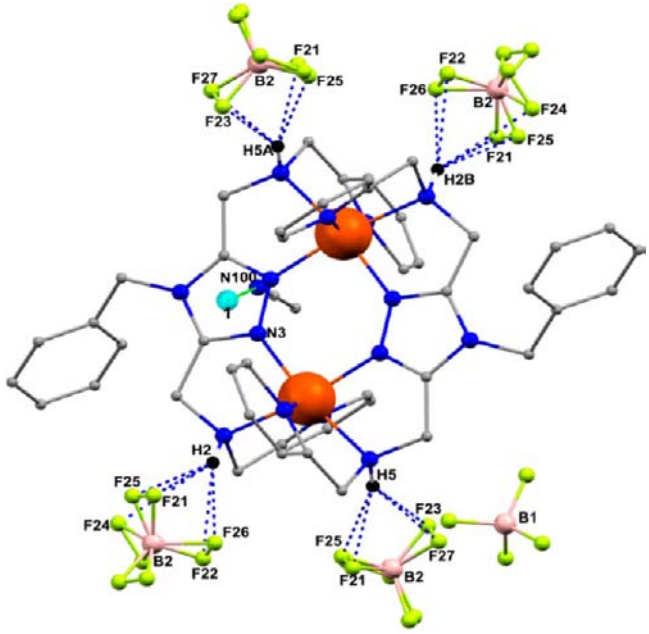

Figure 6. Perspective view of the structure of $[Fe^{II}_2(\mathbf{PMBzT})_2](BF_4)_4$·$CH_3CN$. Color codes: iron, orange spheres; nitrogen, royal blue spheres; oxygen, red spheres; carbon, gray spheres; fluorine, green spheres; boron, tan spheres; and hydrogen, black spheres. H-bonds represented by blue dashed lines, anion−π interactions represented by green dashed lines, and light blue sphere 1 represents ring centroid.

The structure and intermolecular interactions, at 123 K, for $[Fe^{II}_2(\mathbf{PMAT})_2](BF_4)_4$·DMF are depicted in Figures 7 and 8, as the intermolecular interactions were not detailed previously.[15] At 123 K each iron(II) center is trapped in a different spin state [LS is shown as a bright blue sphere and HS as an orange

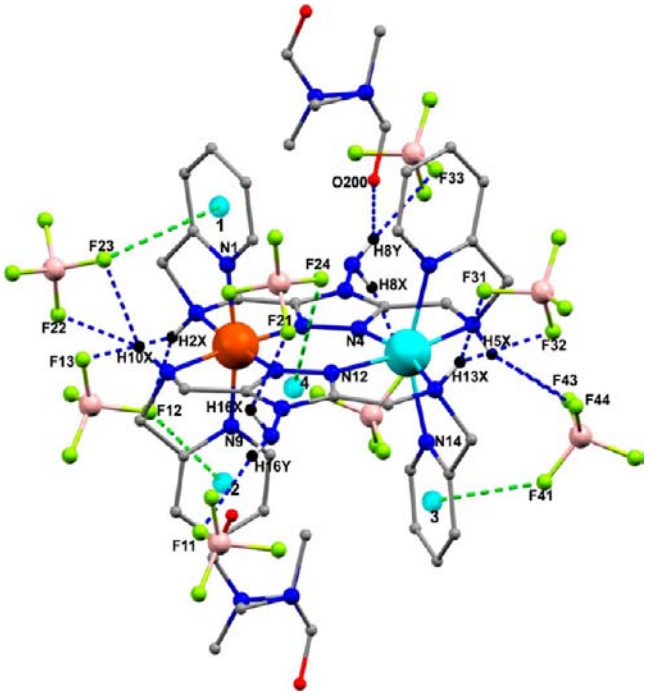

Figure 7. Perspective view of $[Fe^{II}_2(\mathbf{PMAT})_2](BF_4)_4$·DMF at 123 K summarizing H-bonding and anion−π interactions (DMF disordered). Color codes: high spin iron, orange sphere; low spin iron, light blue sphere; nitrogen, royal blue spheres; oxygen, red spheres; carbon, gray spheres; fluorine, green spheres; boron, tan spheres; and hydrogen, black spheres. H-bonds represented by blue dashed lines, anion−π interactions represented by green dashed lines, and light blue spheres marked 1−4 represent ring centroids.

sphere]. This compound forms additional intermolecular interactions, over and above those seen in the previous complexes, due to the presence of the amino group in the N^4-position. Overall the hydrogen bonding pattern extends out in a three-dimensional network (Figure 8 and Supporting Information Figures S16−S18). All of the primary and secondary amine protons make hydrogen bonds [green dashed lines in Figure 7]; H8X, H16X, and H16Y bind to fluorine atoms F21, F41, and F11, respectively, of tetrafluoroborate anions [N−H···F = 3.023(8)−3.246(9) Å and ∠(N−H···F) = 128−159°]. Finally, the proton labeled H8Y binds not only to a tetrafluoroborate fluorine F33 but also to a DMF oxygen O200. Anion−π interactions[29] are observed between the anions hydrogen bonded to the secondary amines and pyridine rings N1 and N9 coordinating the same HS iron center [centroid 1···F23 = 3.326(4) Å and centroid 2···F12 = 3.357(6) Å]. A short interaction occurs between the anion H-bonded to a secondary amine and pyridine ring N14 coordinating to a LS iron center [centroid 3···F41 = 2.980(4) Å]. Also, the triazole ring N12 is interacting with the tetrafluoroborate anion [centroid 4···F24 = 3.298(5) Å]. See Supporting Information, Tables S9 and S10, for full details of the hydrogen bonding and anion−π interactions.

At 123 K the mixed spin state $[Fe^{II}_2(\mathbf{PMAT})_2]^{4+}$ cations are arranged in the lattice such that for both the HS and LS iron(II) centers within this cation the nearest iron(II) center of a neighboring complex is of the same spin state (Figure 8D, light blue lines). This results in chains with a [LS−HS]−[HS−LS]−[LS−HS] pattern of nearest neighbor $[Fe^{II}_2(\mathbf{PMAT})_2]^{4+}$ cation spin states running through the lattice. The second closest neighbor is also of the same spin state (Figure 8D, yellow transparent line), which leads to the parallel alignment of these

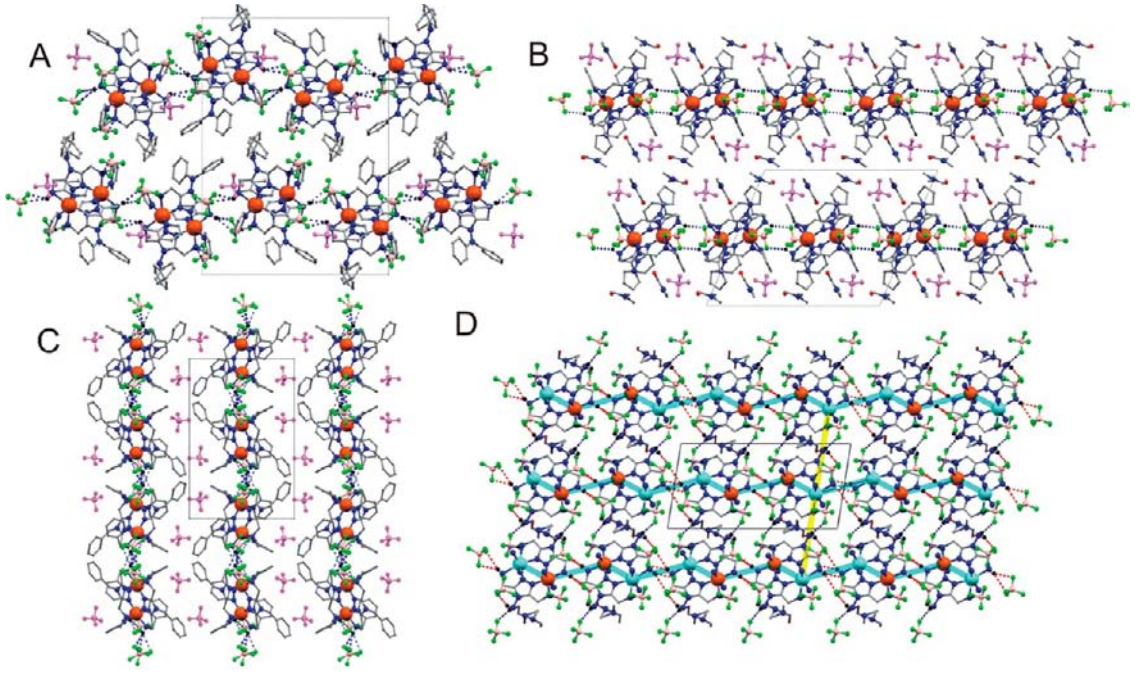

Figure 8. Packing at 90 K of (A) $[Fe^{II}_2(\mathbf{PM^{Ph}AT})_2](BF_4)_4$·solvents along the *a* axis, (B) $[Fe^{II}_2(\mathbf{PMPT})_2](BF_4)_4$·4DMF along the *b* axis, (C) $[Fe^{II}_2(\mathbf{PMBzT})_2](BF_4)_4$·$CH_3CN$ along the *c* axis, and (D) $[Fe^{II}_2(\mathbf{PMAT})_2](BF_4)_4$·DMF at 123 K along the *b* axis with the transparent blue lines showing the chains of −[LS−HS]−[HS−LS]−[LS−HS]− nearest neighbors and the transparent yellow line showing the next nearest neighbors. Pyridine carbon atoms removed for clarity. Atom color codes: HS iron(II), orange; LS iron(II), light blue; nitrogen, royal blue; oxygen, red; carbon, gray; fluorine, green; boron, tan; and N-hydrogen atoms, black spheres. H-bonds represented by blue or red dashed lines. In A−C the BF_4 anions not involved in H-bonds are shown in pink. For additional views, see Supporting Information.

dx.doi.org/10.1021/ic4014416 | *Inorg. Chem.* 2013, 52, 11185−11199

chains. There are hydrogen bonds along (red dashed lines), and between (blue dashed lines), these chains. This three-dimensional hydrogen bonding network and the short contacts, along with the fact that **PMAT** is a highly constrained ligand, are the likely reasons that (a) only half SCO, from [HS−HS] to [HS−LS], is observed (no evidence for [LS−LS] for any PMRT complexes to date, see later), (b) the [HS−LS] state is of the localized type (not 1:1 [LS−LS]:[HS−HS]), and (c) the SCO is abrupt so is better described as an spin transition (ST).

The other three complexes characterized by X-ray crystallography at 90 K are all in the [HS−HS] state, but pack in a similar manner, forming one-dimensional hydrogen bonded chains running parallel to one of the axes (Figure 8). In contrast to $[Fe^{II}_2(\mathbf{PMAT})_2](BF_4)_4\cdot DMF$, half of the BF_4^- counteranions in these three structures are not involved in the hydrogen bonding network (pink in Figure 8), so there are no hydrogen bonds between the 1D-chains.

In all **PMRT** complexes where iron(II) is in the [HS−HS] configuration, the geometries around Fe(II) are very similar. The average *cis*-N−Fe−N angle lies between 90.4° and 90.6° and average *trans*-N−Fe−N angle ranges from 164.3° to 167.1°. However these averages are rather misleading, as the actual values range widely, for example, the *cis*-N−Fe−N lie in the range 75.2(2)−116.0(2)°. The average Fe−N bond distances in these [HS−HS] complexes fall in the range 2.083−2.194 Å as is fairly typical for HS iron(II). In contrast, LS iron(II) centers tend to have shorter Fe−N bonds (as the antibonding e_g orbital is unoccupied) and to be closer to octahedral, and hence have a lower distortion parameter Σ and be more sterically demanding, than HS iron(II) centers. The structure of the mixed spin [HS−LS] $[Fe^{II}_2(\mathbf{PMAT})_2](BF_4)_4\cdot DMF$ complex, at 123 K, provides a very clear illustration of this difference, with an Fe−N bond range 1.934(3)−2.071(4) Å for the LS center versus 2.131(3)−2.319(4) Å for HS, *cis*-N−Fe−N angles of 81.8(1)−101.1(1)° for LS versus 75.1(1)−121.6(1)° for HS, and octahedral distortion parameters of 65.0° for LS versus 133.1° for HS. In fact, as all 12 donors to these two iron(II) centers come from just two highly constrained **PMAT** ligands, the shorter Fe−N bond lengths and being closer to octahedral geometry at the LS center in this complex cause even greater distortions at the HS iron(II) side. This is reflected by the average Fe−N bond lengths in this structure (2.202 Å), *cis*-N−Fe−N angles (75.1−121.6°), and Σ (133.1°) being even higher for this HS iron(II) than is seen in the other three [HS−HS] complexes reported here (Table 1).

Magnetochemistry. Variable temperature (VT) magnetic measurements, 300−2 K, were performed on all seven complexes (Figures 9 and 10 and Supporting Information Figures S19−S25). Five complexes showed SCO behavior, but two, the N^4-pyrrolyl substituted $[Fe^{II}_2(\mathbf{PMPT})_2](BF_4)_4\cdot H_2O$ (Figure 9) and N^4-diphenylamino substituted $[Fe^{II}_2(\mathbf{PM^{Ph}AT})_2](BF_4)_4$ (Figures S19 and S20, Supporting Information), are SCO-inactive, remaining [HS−HS] or mostly [HS−HS], respectively, at all temperatures studied (Table 4). The effective magnetic moments per iron(II) center at room temperature (RT), of 5.03 and 5.14 μ_B, respectively, are in good agreement with the stabilization of the [HS−HS] state (Figure 9). On cooling, these values remain relatively constant until ca. 25 K, below which temperature the magnetic moment decreases due to zero field splitting. These two complexes remaining [HS−HS] is consistent with the structural analysis of their solvatomorphs (above). As expected, the VT magnetic measurements reveal weak antiferromagnetic interactions between the doubly triazole bridged iron(II) centers. The

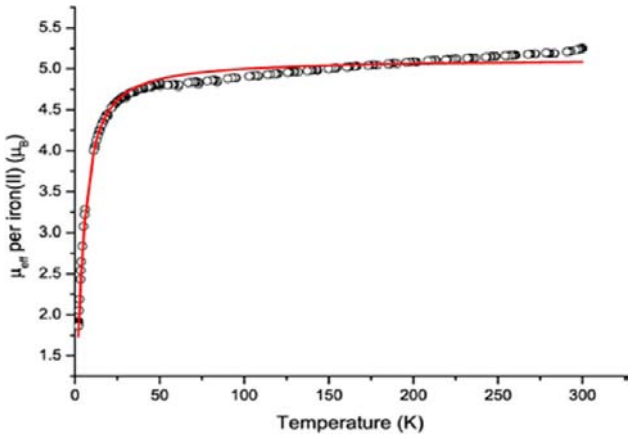

Figure 9. Effective magnetic moment per iron(II) center vs temperature for the [HS−HS] complex $[Fe^{II}_2(\mathbf{PMPT})_2](BF_4)_4\cdot H_2O$ (○) and the calculated fit as described in the text and Table 2 (—).

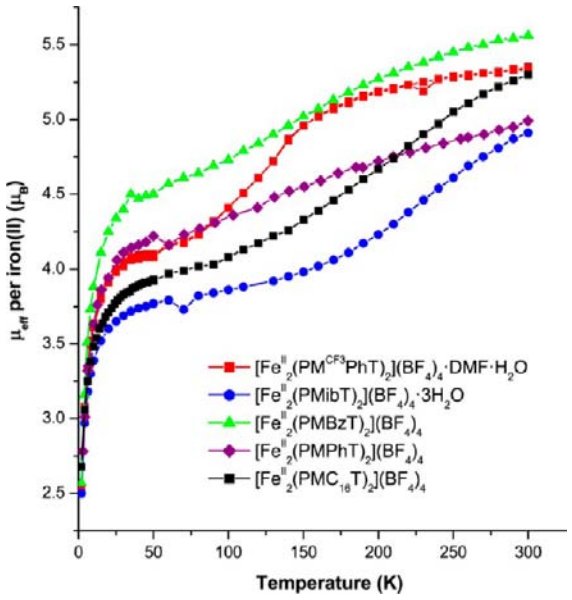

Figure 10. Effective magnetic moment per iron(II) center vs temperature for the SCO-active complexes $[Fe^{II}_2(\mathbf{PM^{CF3}PhT})_2](BF_4)_4\cdot DMF\cdot H_2O$, $[Fe^{II}_2(\mathbf{PMibT})_2](BF_4)_4\cdot 3H_2O$, $[Fe^{II}_2(\mathbf{PMBzT})_2](BF_4)_4$, $[Fe^{II}_2(\mathbf{PMPhT})_2](BF_4)_4$, and $[Fe^{II}_2(\mathbf{PMC_{16}T})_2](BF_4)_4$.

coupling constants, J, for $[Fe^{II}_2(\mathbf{PM^{Ph}AT})_2](BF_4)_4$ and $[Fe^{II}_2(\mathbf{PMPT})_2](BF_4)_4\cdot H_2O$, are −0.61(1) and −1.64(3) cm^{-1}, respectively ($H_{ex} = -J[S_1S_2]$, Table 2), and are similar to those found for the singly triazole bridged diiron(II) complexes previously reported by this research group.[9]

At 300 K, the μ_{eff} values for $[Fe^{II}_2(\mathbf{PMPhT})_2](BF_4)_4$, $[Fe^{II}_2(\mathbf{PMibT})_2](BF_4)_4\cdot 3H_2O$, $Fe^{II}_2(\mathbf{PM^{CF3}PhT})_2](BF_4)_4\cdot DMF\cdot H_2O$, $[Fe^{II}_2(\mathbf{PMBzT})_2](BF_4)_4$, and $[Fe^{II}_2(\mathbf{PMC_{16}T})_2](BF_4)_4$ range between 4.91 and 5.56, broadly consistent with [HS−HS] iron configurations at this temperature (Table 4). For $[Fe^{II}_2(\mathbf{PMibT})_2](BF_4)_4\cdot 3H_2O$ the μ_{eff} drops to 3.77 μ_B per Fe at 50 K, in perfect agreement with fully populated [HS−LS] pairs, and consistent with gradual half-SCO from 90% [HS−HS] at RT to [HS−LS] at 50 K (Figure 10, Table 4). Similarly at 50 K the μ_{eff} value for $[Fe^{II}_2(\mathbf{PMC_{16}T})_2](BF_4)_4$ is 3.92 μ_B per Fe, consistent with the [HS−LS] state: this complex therefore undergoes a reversible, gradual, and complete half-SCO from the [HS−HS] to the [HS−LS] state in the temperature range 300−2 K.

dx.doi.org/10.1021/ic4014416 | *Inorg. Chem.* 2013, 52, 11185−11199

Table 2. Magnetic Parameters Obtained by Fitting the Variable Temperature Magnetic Data Using MAGMUN 4.11[31] for the Two Complexes Stabilized in the [HS−HS] State: $[Fe^{II}_2(PMPT)_2](BF_4)_4{\cdot}H_2O$ and $[Fe^{II}_2(PM^{Ph}AT)_2](BF_4)_4$

compound	spin state 300−2 K	μ per metal center (BM)]at 50 K	g	J^a (cm^{-1})	TIP × 10^6 [cm^3 mol^{-1}]	α	θ (K)	D (ZFS) (cm^{-1})	10^2R
$[Fe^{II}_2(\mathbf{PMPT})_2](BF_4)_4{\cdot}H_2O$	[HS−HS]	4.83	2.090(3)	−1.64(3)	47	0.009	0	2.4	3.17
$[Fe^{II}_2(\mathbf{PM^{Ph}AT})_2](BF_4)_4$	[HS−HS]	5.04	2.082(3)	−0.61(1)	0.5	0.00	0	2.0	1.73

[a]Hamiltonian used to fit the data $H_{ex} = -J[S_1S_2]$; for more details of the fitting procedure, please see the Supporting Information.

At 50 K, $[Fe^{II}_2(\mathbf{PMPhT})_2](BF_4)_4$ and $[Fe^{II}_2(\mathbf{PM^{CF3}PhT})_2](BF_4)_4{\cdot}DMF{\cdot}H_2O$ have μ_{eff} values of 4.22 and 4.08 μ_B per Fe, respectively, consistent with half-SCO, from mostly [HS−HS] and fully [HS−HS], respectively, to mostly the [HS−LS] state. The μ_{eff} value at 50 K for $[Fe^{II}_2(\mathbf{PMBzT})_2](BF_4)_4$ is 4.50 μ_B per Fe which is significantly higher than the expected 3.50 μ_B per Fe for a dinuclear iron(II) complex in the [HS−LS] state, suggesting that the half-SCO is incomplete (see below). The magnetic moment data in Figures 9 and 10, and Supporting Information Figures S19−S25, was mainly collected on cooling, but it was essentially reversible on heating (see Supporting Information Figure S23 for $[Fe^{II}_2(\mathbf{PM^{CF3}PhT})_2](BF_4)_4{\cdot}DMF{\cdot}H_2O$). In summary, the VT magnetic data is consistent with five of these seven complexes undergoing a gradual half-SCO involving the [HS−HS] and [HS−LS] states, with $T_{1/2}$ values of 234, 224, 133, 147, and 187 K for $[Fe^{II}_2(\mathbf{PMibT})_2](BF_4)_4{\cdot}3H_2O$, $[Fe^{II}_2(\mathbf{PMC_{16}T})_2](BF_4)_4$, $[Fe^{II}_2(\mathbf{PM^{CF3}PhT})_2](BF_4)_4{\cdot}DMF{\cdot}H_2O$, $[Fe^{II}_2(\mathbf{PMBzT})_2](BF_4)_4$, and $[Fe^{II}_2(\mathbf{PMPhT})_2](BF_4)_4$, respectively (Figure 10 and Supporting Information Figures S21−S25). This compares with the abrupt half-SCO between the [HS−HS] and localized [HS−LS] state, observed at 224 K for $[Fe^{II}_2(\mathbf{PMAT})_2](BF_4)_4{\cdot}DMF$ (for which μ_{eff} per Fe is 5.2 μ_B at 300 K and 3.8 μ_B in the plateau region).[15]

Mössbauer Spectroscopy. All seven complexes presented in this work were studied by ^{57}Fe Mössbauer spectroscopy. The spectra collected at ∼5 K together with fits using either Lorentzian or Voigt line shapes are presented in Figure 11, and parameters are given in Table 3. All spectra showed characteristic quadrupole doublets corresponding to HS (red line) and LS (blue line) iron centers. The isomer shifts and quadrupole splitting parameters for HS iron(II) at ∼5 K range narrowly between 1.09 and 1.1 mm s^{-1} and between 2.56 and 2.87 mm s^{-1}, respectively. This is in good agreement with previously reported values for HS iron(II) in similar systems **PMAT** and **HdiPMAP**.[2,15,32,33] The isomer shifts decrease consistently by ∼0.15 mm s^{-1} when the temperature is raised to ca. 295 K (see Table S12 in the Supporting Information) which is due to the second order Doppler shift.[34]

The quadrupole splitting of HS centers also decreases (0.3 mm s^{-1}) as is commonly observed in SCO compounds.[33,35] The low temperature Mössbauer data show that LS iron(II) have isomer shifts in the range 0.40−0.51 mm s^{-1} and quadrupole splitting between 0.21 and 0.30 mm s^{-1}. The room temperature LS iron(II) signals were very weak, and therefore, paramaters were only assigned to the HS iron(II) at this temperature.

By analogy to our study[33] of the effect of the choice of counteranion on the SCO properties of $[Fe^{II}_2(\mathbf{PMAT})_2]^{4+}$, we again compare the information on iron(II) spin state obtained from the magnetic measurements to that obtained from careful curve fitting of the Mössbauer data (Table 4). The low temperature values of LS iron(II) fraction obtained from Mössbauer and magnetic measurements are, on the whole, in excellent agreement with each other.[36,37]

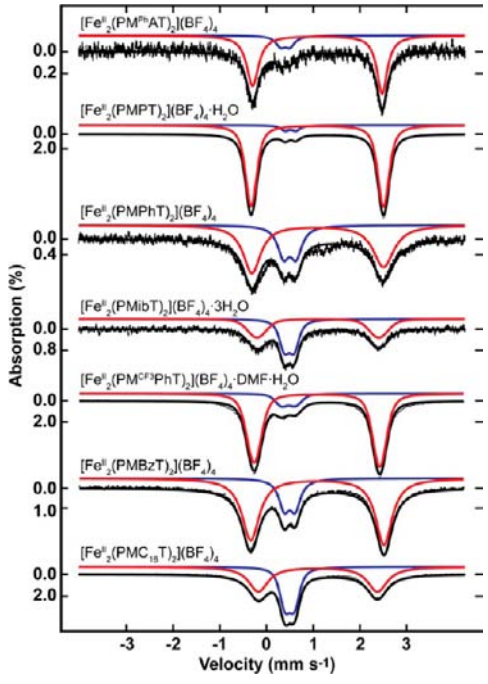

Figure 11. ^{57}Fe Mössbauer spectra of the complexes reported in this work measured at 5 K. Spectra are deconvoluted into quadrupole doublets corresponding to HS Fe^{II} (red line) and LS Fe^{II} (blue line).

CONCLUSIONS

A convenient and general (applicable to any primary amine) four step route to highly constrained bis-terdentate triazole-based **PMRT** ligands has been successfully developed. By employing this route, seven **PMRT** ligands have been prepared and then complexed with iron(II). The resulting family of dimetallic complexes, $[Fe^{II}_2(\mathbf{PMRT})_2](BF_4)_4$, varies in the nature of the N^4 substituent on the triazole moiety. The effect of this variation on the spin state of the two iron(II) centers was investigated by variable temperature magnetic susceptibility measurements and Mössbauer spectroscopy and where possible also by single crystal X-ray crystallography.

While the substituent R is relatively remote from the iron(II) binding sites, it was fully anticipated that the properties of $[Fe^{II}_2(\mathbf{PMRT})_2](BF_4)_4$ would be highly dependent on the nature of R, not least as it will affect packing. Indeed no SCO occurred when the N^4-nitrogen atom was attached to another nitrogen atom in the form of a tertiary amine, in $[Fe^{II}_2(\mathbf{PM^{Ph}AT})_2](BF_4)_4$, or a pyrrolyl, in $[Fe^{II}_2(\mathbf{PMPT})_2](BF_4)_4{\cdot}H_2O$. In contrast, when the N^4-nitrogen atom was attached to the carbon atom of an aromatic substituent, such as phenyl in $[Fe^{II}_2(\mathbf{PMPhT})_2](BF_4)_4$ and trifluoromethyl phenyl in $[Fe^{II}_2(\mathbf{PMCF_3PhT})_2](BF_4)_4{\cdot}DMF{\cdot}H_2O$, gradual and incomplete half-SCO was observed. When N^4 was connected to alkyl groups, isobutyl in $[Fe^{II}_2(\mathbf{PMibT})_2](BF_4)_4{\cdot}3H_2O$ and hexadecyl in $[Fe^{II}_2(\mathbf{PMC_{16}T})_2](BF_4)_4$, the resulting complexes showed gradual and

dx.doi.org/10.1021/ic4014416 | Inorg. Chem. 2013, 52, 11185−11199

Table 3. Mössbauer Parameters of the Iron(II) Complexes Measured at ca. 5 K

complex	T (K)	species	δ (mm s^{-1})	ΔE_Q (mm s^{-1})	$\Gamma_{L/R}$ (mm s^{-1})	I (%)
$[Fe^{II}_2(\mathbf{PM^{Ph}AT})_2](BF_4)_4$	5.1	HS	1.09	2.77	0.31/0.27	86
		LS	0.40	0.20	0.25/0.25	14
$[Fe^{II}_2(\mathbf{PMPT})_2](BF_4)_4{\cdot}H_2O$	5.1	HS	1.09	2.83	0.20/0.20[a]	95
		LS	0.51	0.23	0.22/0.22	5
$[Fe^{II}_2(\mathbf{PMPhT})_2](BF_4)_4$	5.5	HS	1.10	2.82	0.45/0.53	71
		LS	0.50	0.27	0.30/0.30	29
$[Fe^{II}_2(\mathbf{PMibT})_2](BF_4)_4{\cdot}3H_2O$	5.2	HS	1.11	2.62	0.46/0.46[a]	52
		LS	0.49	0.21	0.15/0.15[a]	48
$[Fe^{II}_2(\mathbf{PM^{CF3}PhT})_2](BF_4)_4{\cdot}DMF{\cdot}H_2O$	5.2	HS	1.09 (1.09[b])	2.70 (2.69[b])	0.33/0.30[a] (0.37/0.34[a,b])	87 (81[b])
		LS	0.47 (0.49[b])	0.30 (0.30[b])	0.25/0.26[a] (0.21/0.20[a,b])	13 (19[b])
$[Fe^{II}_2(\mathbf{PMBzT})_2](BF_4)_4$	5.8	HS	1.09	2.87	0.46/0.43	78
		LS	0.5	0.24	0.27/0.27	22
$[Fe^{II}_2(\mathbf{PMC_{16}T})_2](BF_4)_4$	5.1	HS	1.11	2.56	0.51/0.52	59
		LS	0.50	0.21	0.17/0.17[a]	41

[a]Voigt line shape was used to fit these spectra. [b]Measured one month later at 5.3 K.

Table 4. Comparison of the Spin State Information (Provided as an Approximate HS/LS Ratio) Obtained from the Mössbauer and Magnetic Studies

complex	5 K (Mössbauer)[a]	50 K (magnetic)[b]	300 K (magnetic)[b,c]
$[Fe^{II}_2(\mathbf{PM^{Ph}AT})_2](BF_4)_4$	86:14	90:10	91:9
$[Fe^{II}_2(\mathbf{PMPT})_2](BF_4)_4{\cdot}H_2O$	95:5	85:15	100:0
$[Fe^{II}_2(\mathbf{PMPhT})_2](BF_4)_4$	71:29	64:36	90:10
$[Fe^{II}_2(\mathbf{PMibT})_2](BF_4)_4{\cdot}3H_2O$	52:48	51:49	87:13
$[Fe^{II}_2(\mathbf{PM^{CF3}PhT})_2](BF_4)_4{\cdot}DMF{\cdot}H_2O$	81:19[36]	60:40	100:0
$[Fe^{II}_2(\mathbf{PMBzT})_2](BF_4)_4$	78:22	73:27	100:0
$[Fe^{II}_2(\mathbf{PMC_{16}T})_2](BF_4)_4$	59:41	55:45	100:0

[a]Approximate HS/LS ratio as obtained from fitting the Mössbauer data. [b]Approximate HS/LS ratio calculated from the magnetic data as follows (note that the range either side of this is large, see the following description and the Supporting Information). The accepted range of μ_{eff} per HS iron(II) is 5.0−5.6 μB. Hence 5.0 and 5.6 μB were each converted to χT values per iron, then to χT values for a [HS−HS] dimer and for a [LS−HS] dimer (half the previous value). This gave us a linear function of %HS vs χT for both values of μ_{eff}. These lines were used to calculate the %HS from the experimental data along with an estimate of the error associated with this value (see Supporting Information). [c]Mössbauer spectra measured at room temperature had a very low % effect. Additionally, the amount of LS was very small; therefore, parameters for the LS and the relative proportions of HS/LS could not be determined with confidence from the Mössbauer spectra, and only magnetic measurements were used.

complete half-SCO, and incomplete half-SCO for benzyl in $[Fe^{II}_2(\mathbf{PMBzT})_2](BF_4)_4$. In summary, we have demonstrated that the magnetic behavior of this family of complexes is indeed highly dependent on the choice of R, most likely primarily due to the effect that varying this substituent has on the solvent content and packing.

Having developed a reliable and general route to N^4-substituted bis-terdentate **PMRT** ligands, we are now employing this to investigate the effect of incorporating additional functionality at the N^4-position. We are also using some of the intermediates generated in this synthetic route to gain access to new classes of interesting 3,5-disubstituted triazole ligands, that feature our choice of N^4-substituent, denticity, and functional groups.

EXPERIMENTAL SECTION

N,*N*-Dimethylformamide azine was prepared according to the literature method.[17] Syntheses of N^4-amino-3,5-bis-hydroxymethyl-1,2,4-triazole (**2a**), N^4-amino-3,5-bis-chloromethyl-1,2,4-triazole (**3a**), N^4-pyrrolyl-3,5-bis-chloromethyl-1,2,4-triazole (**3b**), and N^4-amino-3,5-bis{[(2-pyridylmethyl)amino]methyl}-4*H*-1,2,4-triazole (**PMAT**) were reported previously.[14] Primary amines, paraformaldehyde, thionylchloride, and $Fe(BF_4)_2{\cdot}6H_2O$ were all purchased from commercial sources and used as received. All solvents were laboratory reagent grade except methanol, acetonitrile, and pyridine. Methanol was HPLC grade and used as received. Acetonitrile and pyridine were dried by freshly distilling over calcium hydride before use. Elemental analyses were carried out by the Campbell Microanalytical Laboratory at the University of Otago. Infrared spectra were recorded over the range 4000−400 cm^{-1} with a Perkin-Elmer Spectrum NBX FT-IR spectrophotometer as a potassium bromide pellet or on a Bruker Alpha FT-ATR with an Alpha-P module. ^{1}H and ^{13}C{^{1}H} NMR spectra were recorded on either a Varian INOVA-500, a Varian INOVA-300, a Varian 400-MR, or a Varian 500 MHz VNMRS spectrometer at 25 °C and referenced to residual solvent signals.[38] Magnetic data were recorded over the range 300−2 K with a Quantum Design MPMS5 SQUID or PPMS with an applied field of 0.1 or 1 T by J.L.T. and J.A.K., J.O., or V.A.M. at Industrial Research Limited (IRL). ESI mass spectra were recorded on a Bruker MicrOTOF$_Q$ spectrometer by Mr. Ian Stewart at the University of Otago. ^{57}Fe Mössbauer spectra were recorded at the University of Otago on a SEE Co. (Science Engineering & Education Co., MN) Mössbauer spectroscopy system by G.N.L.J. X-ray data were collected using a Bruker APEX II area detector diffractometer at the University of Otago, using graphite-monochromated Mo Kα radiation (λ = 0.710 73 Å). The data were corrected for Lorentz and polarization effects, and semiempirical absorption corrections (SCALE) were applied.[39] The structures were solved by direct methods (SHELXS-97) and refined against all F^2 data (SHELXL-97).[40] Hydrogen atoms, except those attached to oxygen or nitrogen atoms which were typically fixed and allowed to freely refine, were inserted at calculated positions and rode on the atoms to which they were attached. All non-hydrogen atoms were refined anisotropically. For further crystallography details please see the Supporting Information. High resolution pictures were prepared using Mercury[41] and POVray[42] software.

dx.doi.org/10.1021/ic4014416 | Inorg. Chem. 2013, 52, 11185−11199

Organic Synthesis. See Figure S27 in the Supporting Information for the atom numbering scheme used for NMR assignments.

General Procedure for Preparation of N⁴-Substituted-1,2,4-triazoles (1). *N,N*-Dimethylformamide azine dihydrochloride (1.5 equiv) and the primary amine (1 equiv) were refluxed in pyridine (~50 mL) for 24–48 h. On cooling to room temperature a colorless crystalline solid formed. The pyridine was removed in vacuo, and trace amounts azeotroped with toluene (50 mL) to give an orange-yellow oily solid. This was taken up in methanol (50 mL) to give a clear yellow solution. The methanol was removed in vacuo and the oily solid then taken up in dichloromethane (50 mL), once again giving a clear yellow solution. This solution was washed with water (50 mL), $NaHCO_3$ (sat. aq, 50 mL), and NaCl (sat. aq, 50 mL) before drying over Na_2SO_4 and removing the solvent. Recrystallizing the resulting solids (typically off-white/yellow) from toluene gave the analytically pure triazoles (**1c**–**1h**).

N⁴-(N,N-Diphenylamine)-1,2,4-triazole (1c). The reaction of *N,N*-dimethylformamide azine dihydrochloride (4.00 g, 18 mmol) and *N,N′*-diphenyl hydrazine hydrochloride (2.73 g, 12 mmol) according to the general procedure gave the desired product as an off-white solid (1.78 g, 61%). Anal. Calcd for $C_{12}H_{14}N_4$ (236.11 g mol^{-1}): C 71.15, H 5.12, N 23.72. Found: C 71.22, H 5.04, N 24.03%. δ_H (300 MHz, $CDCl_3$): 6.93 (d, 4H, 7.6 Hz, H^3), 7.17 (t, 2H, 7.4 Hz, H^5),7.34 (t, 4H, 7.9 Hz, H^4), 8.42 (s, 2H, H^1). δ_C (75 MHz, $CDCl_3$): 120.9 (C^3), 125.1 (C^5), 129.3 (C^4), 143.1 (C^2), 145.1 (C^1). IR (ATR): 3255, 3087, 1586, 1491, 1457, 1310, 1156, 1056, 1024, 1001, 971, 886, 743, 689, 658, 501, 455 cm^{-1}.

N⁴-Phenyl-1,2,4-triazole (1d). The reaction of *N,N*-dimethylformamide azine dihydrochloride (19.40 g, 90 mmol) and aniline (6.98 g, 75 mmol) according to the general procedure gave the desired product as colorless flakes (8.41 g, 77%). Anal. Calcd for $C_8H_7N_3$ (145.16 g mol^{-1}): C 66.19, H 4.86, N 28.95. Found: C 66.21, H 4.87, N 29.06%. δ_H (300 MHz, $CDCl_3$): 7.38–7.41 (m, 2H, H^3), 7.46–7.50 (m, 1H, H^5), 7.52–7.57 (m, 2H, H^4), 8.48 (s, 2H, H^1). δ_C (75 MHz, solvent $CDCl_3$, reference $CDCl_3$ at 77.16 ppm): 122.4 (C^3), 129.2 (C^5), 130.5 (C^4), 134.0 (C^2), 141.6 (C^1). IR (KBr): 3118, 1658, 1589, 1520, 1494, 1365, 1299, 1267, 1223, 1093, 1003, 991, 946, 923, 843, 772, 694, 424 cm^{-1}.

N⁴-3,5-Bis-trifluoromethyl-phenyl-1,2,4-triazole (1e). *N,N*-Dimethylformamide azine dihydrochloride (6.00 g, 28 mmol) and 3,5-di(trifluoromethyl) aniline (4.26 g, 18.6 mmol) were reacted according to the general procedure; however, after reflux for 24 h a second portion of *N,N*-dimethylformamide azine dihydrochloride (6.00 g, 28 mmol) was added, and reflux was continued for 24 h (total reflux time of 48 h). After following the typical workup the result was an orange oil, rather than an off-white solid. The orange oil (which contained unreacted 3,5-di(trifluoromethyl)aniline) was dissolved in 50 mL of diethyl ether, and to this orange solution was added 200 mL of petroleum ether (40–60° bp), giving a light yellow solid. The solid was dried under vacuum resulting in 2.29 g in 44% yield. Anal. Calcd for $C_{10}H_5N_3F_6$ (281.16 g mol^{-1}): C 42.72, H 1.79, N 14.95. Found: C 42.72, H 1.89, N 14.98. δ_H (300 MHz, $CDCl_3$): 7.91 (s, 2H, H^3), 8.01 (s, 1H, H^5), 8.60 (s, 2H, H^1). IR (KBr): 3448, 3346, 3086, 3033, 1692, 1627, 1522, 1474, 1406, 1328, 1277, 1148, 998, 973, 949, 894, 858, 845, 797, 727, 707, 628, 645, 632, 609, 528, 476, 424 cm^{-1}.

N⁴-Benzyl-1,2,4-triazole (1f). The reaction of *N,N*-dimethylformamide azine dihydrochloride (10 g, 46 mmol) and benzyl amine (3.27 g, 31 mmol) according to the general procedure gave the desired product as a yellow solid (3.75 g, 77%). Anal. Calcd for $C_9H_9N_3$ (159.09 g mol^{-1}): C 67.91, H 5.70, N 26.40. Found: C 67.97, H 5.90, N 26.62%. δ_H (500 MHz, $CDCl_3$): 5.19 (s, 2H, H^2), 7.19 (dd, 2H, 2 and 7 Hz, H^5), 7.39 (m, 3H, H^4 and H^6), 8.16 (s, 2H, H^1). δ_C (125 MHz, $CDCl_3$): 48.9 (C^2), 127.6 (C^4), 127.7 (C^6), 128.2 (C^5), 134.3 (Bz-C^3), 142.9 (C^1). IR (KBr disk): 3079, 1678, 1584, 1533, 1453, 1379, 1337, 1306, 1207, 1181, 1075, 1030, 975, 957, 892, 840, 816, 768, 712, 638, 577, 460 cm^{-1}.

N⁴-iso-Butyl-1,2,4-triazole (1g). The reaction of *N,N*-dimethylformamide azine dihydrochloride (8.84 g, 41 mmol) and iso-butyl amine (2.00 g, 27 mmol) according to the general procedure gave the desired product as a colorless crystalline solid (2.12 g, 63%). Anal. Calcd for $C_6H_{11}N_3$ (125.17 g mol^{-1}): C 57.57, H 8.86, N 33.57. Found: C 57.63, H 9.12, N 33.65%. δ_H (300 MHz, $CDCl_3$): 0.89 (d, 6H, 6 Hz, H^4), 2.01 (m, 1H, H^3), 3.79 (d, 7 Hz, H^2), 8.09 (s, 2H, H^1). δ_C (75 MHz, $CDCl_3$): 19.6 (C^4), 29.8 (C^3), 52.6 (C^2), 143.0 (C^1). IR (KBr): 3092, 2957, 2873, 1792, 1718, 1670, 1636, 1528, 1465, 1388, 1363, 1329, 1301, 1233, 1231, 1187, 1118, 1079, 973, 951, 927, 895, 863, 821, 739, 645, 427 cm^{-1}.

N⁴-Hexadecyl-1,2,4-triazole (1h). The reaction of *N,N*-dimethylformamide azine dihydrochloride (2.70 g, 12 mmol) and hexadecyl amine (2.00 g, 8 mmol) according to the general procedure gave the desired product as a white solid (1.70 g, 70%). Anal. Calcd for $C_{18}H_{35}N_3$ (293.49 g mol^{-1}): C 73.66, H 12.02, N 14.32. Found: C 73.49, H 12.01, N 14.03%. δ_H (300 MHz, $CDCl_3$): 0.86 (s, 3H, 7 Hz, H^{17}), 1.23 (br m, 26H, H^{4-16}), 1.79 (m, 2H, 7 Hz, H^3), 3.99 (t, 2H, 7 Hz, H^2), 8.16 (s, 2H, H^1). δ_C (75 MHz, $CDCl_3$): 14.2 (C^{17}), 22.8–32.0 (C^{3-16}), 45.5 (C^2), 142.8 (C^1). IR (KBr): 3098, 2916, 2848, 1717, 1533, 1471, 1390, 1339, 1193, 1079, 982, 958, 882, 733, 718, 642, 447 cm^{-1}.

General Procedure for Preparation of N⁴-Substituted-3,5-bis-hydroxymethyl-1,2,4-triazoles (2). N^4-Substituted-1,2,4-triazole (1 equiv) was dissolved in xylenes (~80–100 mL) with heating to 110 °C. The resulting clear colorless solution was placed under an inert argon atmosphere, and paraformaldehyde (10 equiv) was quickly added by briefly removing the condenser, while argon was flowed into the reaction vessel. The resulting suspension was heated at 125 °C with stirring for 2 h before a second portion of paraformaldehyde (10 equivalents) was added. After 6–8 h of heating (total) the product had precipitated. After cooling the mixture to room temperature the solid was filtered off. The major contaminant in the solid obtained was the monohydroxymethylated compound, but in some cases, residual paraformaldehyde had to be removed too. Purification methods differed for each compound and were dependent on the nature of the headgroup, so these are detailed below. The product was obtained as a pale off-white solid in each case.

N⁴-(N,N-Diphenylamine)-3,5-bis-hydroxymethyl-1,2,4-triazole (2c). The reaction of **1c** (0.93 g, 3.9 mmol) with 2 × 1.18 g (39 mmol) of paraformaldehyde according to the general procedure gave the desired product as a white solid (0.90 g, 77%), by filtration of the cooled (RT) reaction solution. No further purification was necessary. Anal. Calcd for $C_{16}H_{16}N_4O_2$ (294.33 g mol^{-1}): C, 64.85; H, 5.44; N, 18.91. Found: C 64.75; H, 5.58; N, 18.87%. δ_H (300 MHz, d_6-DMSO): 4.28 (d, 4H, 5.8 Hz, H^1), 5.61 (t, 2H, 5.8 Hz, 2 × OH), 7.00 (d, 4H, 7.7 Hz, H^4), 7.10 (t, 2H, 7.3 Hz, H^6), 7.34 (t, 4H, 7.3 Hz, H^5). δ_C (75 MHz, d_6-DMSO): 52.9 (C^1), 118.9 (C^4), 123.7 (C^6), 129.5 (C^5), 143.2 (C^3), 154.5 (C^2). IR (ATR): 3254, 3054, 1589, 1492, 1440, 1293, 1101, 1053, 1022, 928, 885, 746, 719, 697, 622, 518, 498 cm^{-1}

N⁴-Phenyl-3,5-bis-hydroxymethyl-1,2,4-triazole (2d). The reaction of **1d** (1.95 g, 13 mmol) with 2 × 3.90 g (0.13 mol) of paraformaldehyde according to the general procedure gave the desired product as a white solid (1.80 g, 67%) by filtration of the hot reaction solution. No further purification was necessary. Anal. Calcd for $C_{10}H_{11}N_3O_2$ (205.21 g mol^{-1}): C, 58.53; H, 5.40; N, 20.48. Found: C 58.51, H 5.55, N 20.42%. δ_H (300 MHz, d_6-DMSO): 4.41 (d, 4H, 3.3 Hz, H^1), 5.41 (t, 2H, 3.3 Hz OH), 7.50–7.59 (m, 5H, H^{4-6}). δ_C (75 MHz, d_6-DMSO): 53.2 (C^1), 129.2 (C^5), 129.3 (C^6), 129.4 (C^4), 133.7 (C^3), 154.5 (C^2). IR (KBr): 3205, 2861, 1596, 1510, 1442, 1342, 1319, 1296, 1213, 1203, 1181, 1083, 1058, 1025, 998, 977, 943, 825, 772, 737, 694, 541, 454, 421 cm^{-1}.

N⁴-3,5-Bis-trifluoromethylphenyl-3,5-bis-hydroxymethyl-1,2,4-triazole (2e). The reaction of **1e** (0.605 g, 2.15 mmol) with 4 × 0.646 g (21.5 mmol) of paraformaldehyde according to the general procedure gave the desired product as a white solid (0.403 g, 55%) by filtration of the hot (~100 °C) xylenes reaction solution. Anal. Calcd for $C_{12}H_9F_6N_3O_2$ (341.21 g mol^{-1}): C 42.24, H 2.66, N 12.32. Found: C 42.40, H 2.70, N 12.28. δ_H (300 MHz, d_6-DMSO): 4.48 (d, 4H, 6 Hz, H^1), 5.46 (t, 2H, 6 Hz, OH), 8.34 (s, 1H, H^6), 8.37 (s, 2H, H^4). IR (KBr): 3241, 2937, 1630, 1518, 1482, 1447, 1386, 1341, 1274, 1213, 1172, 1129, 1061, 1028, 978, 906, 848, 822, 811, 704, 680, 629, 534, 460, 423 cm^{-1}.

N⁴-Benzyl-3,5-bis-hydroxymethyl-1,2,4-triazole (2f). The reaction of **1f** (3.75 g, 23 mmol) with 2 × 7.00 g (0.23 mol) of paraformaldehyde according to the general procedure gave a yellow waxy

dx.doi.org/10.1021/ic4014416 | *Inorg. Chem.* 2013, 52, 11185–11199

substance. Decanting off the xylenes and crystallizing this waxy solid from water gave the desired product as a white solid (2.73 g, 54%). Anal. Calcd for $C_{11}H_{13}N_3O_2$ (219.24 g mol^{-1}): C, 60.26; H, 5.98; N, 19.17. Found: C, 60.01; H, 6.12; N, 18.96%. δ_H (500 MHz, d_6-DMSO): 4.51 (d, 4H, 5.5 Hz, H^1), 5.39 (s, 2H, H^3), 5.63 (t, 2H, 5.5 Hz OH), 7.21 (m, 2H, 7 Hz, H^6), 7.34 (d, 1H, 7 Hz, H^7), 7.39 (d, 2H, H^5). δ_C (125 MHz, d_6-DMSO): 46.1 (C^3), 53.8 (C^1), 126.8 (C^5), 127.7 (C^7), 128.6 (C^6), 136.0 (C^4), 154.6 (C^2). IR (KBr): 3229, 3088, 1605, 1548, 1463, 1399, 1298, 1202, 1162, 1102, 1043, 1018, 963, 939, 909, 799, 785, 762, 733, 721, 705, 691, 473, 457 cm^{-1}.

*N^4-iso-Butyl-3,5-bis-hydroxymethyl-1,2,4-triazole (**2g**).* The reaction of **1g** (0.60 g, 4.8 mmol) with 2 × 1.44 g (48 mmol) of paraformaldehyde according to the general procedure gave the desired product as a white solid (0.609 g, 69%) by filtration of the hot (~100 °C) reaction solution. Anal. Calcd for $C_8H_{15}N_3O_2$ (185.22 g mol^{-1}): C, 51.88; H, 8.16; N, 22.69. Found: C, 51.71; H, 8.24; N, 22.52%. δ_H (300 MHz, d_6-DMSO,): 0.85 (d, 6H, 6 Hz, H^5), 2.19 (m, 1H, H^4), 3.91 (d, 2H, 6 Hz, H^3), 4.57 (d, 4H, 5 Hz, H^1), 5.55 (t, 2H, 5 Hz, OH). δ_C (75 MHz, d_6-DMSO): 19.6 (C^5), 28.3 (C^4), 49.8 (C^3), 53.9 (C^1), 154.6 (C^2). IR (KBr): 3119, 2965, 1521, 1466, 1369, 1211, 1158, 1092, 1060, 1041, 1013, 884, 803, 784, 658, 575 cm^{-1}.

*N^4-Hexadecyl-3,5-bis-hydroxymethyl-1,2,4-triazole (**2h**).* The reaction of **1h** (1.00 g, 3.4 mmol) with 2 × 1.00 g (34 mmol) of paraformaldehyde according to the general procedure gave the desired product as a white solid (0.56 g, 46%), by filtration of the cooled (RT) reaction solution. No further purification was necessary. Anal. Calcd for $C_{20}H_{39}N_3O_2$ (353.54 g mol^{-1}): C, 67.94; H, 11.12; N, 11.89. Found: C 67.77; H, 11.33; N, 11.65%. δ_H (300 MHz, d_6-DMSO): 0.86 (t, 3H, 6.6 Hz, H^{18}), 1.25 (m, br, 26H, H$^{5-17}$), 1.74 (m, 2H, 7.7 Hz, H^4), 4.03 (t, 2H, 7.8 Hz H^3), 4.57 (d, 4H, 5.7 Hz, H^1), 5.53 (t, 2H, 5.7 Hz, OH). δ_C (75 MHz, d_6-DMSO): 13.9 (C^{18}), 22.1−31.3 (C$^{4-17}$), 43.1 (C^3) 53.7 (C^1), 154.3 (C^2). IR (KBr): 3224, 2914, 2848, 1518, 1471, 1398, 1353, 1254, 1198, 1049, 1025, 968, 829, 818, 718, 491, 463 cm^{-1}.

*General Procedure for Preparation of N^4-Substituted-3,5-bis-chloromethyl-1,2,4-triazoles and Triazole Hydrochlorides (**3**).* The N^4-substituted-3,5-bis-hydroxymethyl-1,2,4-triazole was dissolved in an excess of thionyl chloride, resulting in a vigorous exothermic reaction. The resulting yellow solution was left to stir, open to the air, until the excess thionyl chloride had evaporated, leaving a pale yellow solid. Drying the solid in vacuo and then crystallizing it from absolute ethanol gave the desired products (**3c**−**3h**) as crystalline solids.

*N^4-(N,N-Diphenylamine)-3,5-bis-chloromethyl-1,2,4-triazole (**3c**).* The reaction of **2c** (0.9 g, 3.0 mmol) and 10 mL of $SOCl_2$ according to the general procedure gave the desired product **3c** as a colorless crystalline solid (0.65 g, 64%). Anal. Calcd for $C_{16}H_{14}N_4Cl_2$ (333.22 g mol^{-1}): C 57.67, H 4.23, N 16.81. Found: C 57.67, H 4.26, N 16.86%. δ_H (300 MHz, d_6-DMSO): 4.68 (s, 4H, H^1), 7.00 (d, 4H, 7.8 Hz, H^4), 7.16 (t, 2H, 7.4 Hz, H^6), 7.39 (t, 4H, 7.8 Hz, H^5). δ_C (75 MHz, d_6-DMSO): 32.6 (C^1), 119.0 (C^4), 124.5 (C^6), 129.8 (C^5), 142.5 (C^3), 152.1 (C^2). IR (KBr): 3443, 3068, 1568, 1488, 1429, 1270, 1244, 1175, 1024, 921, 884, 668, 620, 575, 509, 484 cm^{-1}.

*N^4-Phenyl-3,5-bis-chloromethyl-1,2,4-triazole hydrochloride (**3d**).* The reaction of **2d** (1.00 g, 4.9 mmol) and 10 mL of $SOCl_2$ according to the general procedure gave the desired product as large pale brown crystals (1.35 g, 98%). Anal. Calcd for $C_{10}H_{10}N_3C_{l3}$ (278.57 g mol^{-1}): C 43.12, H 3.62, N 15.08. Found: C 43.35, H 3.70, N 15.13%. δ_H (300 MHz, d_6-DMSO): 4.74 (s, 4H, H^1), 7.56−7.66 (m, 5H, H$^{4-6}$). δ_C (75 MHz, d_6-DMSO): 33.9 (C^1), 127.2 (C^3), 130.0 (C^5), 130.4 (C^6), 132.1 (C^4), 152.2 (C^2). IR (KBr): 3072, 3012, 2959, 2166, 1839, 1581, 1546, 1525, 1458, 1424, 1385, 1356, 1291, 1260, 1242, 1145, 1101, 1074, 1049, 1014, 947, 914, 891, 802, 764, 753, 721, 671, 613, 544, 454, 409 cm^{-1}.

*N^4-3,5-Bis-trifluoromethylphenyl-3,5-bis-chloromethyl-1,2,4-triazole (**3e**).* The reaction of **2e** (0.40 g, 1.2 mmol) and 10 mL of $SOCl_2$ according to the general procedure gave the desired product as a colorless crystalline solid (0.30 g, 66%). Anal. Calcd for $C_{12}H_7N_3Cl_2F_6 \cdot {}^2/_3HCl$ (378.10 g mol^{-1}): C 35.85, H 1.98, N 10.44. Found: C 35.74, H 2.04, N 10.35%. δ_H (300 MHz, d_6-DMSO): 4.84 (s, 4H, H^1), 8.46 (s, 1H, H^6), 8.49 (s, 2H, H^4). IR (KBr): 3038, 2487, 1883, 1627, 1587, 1551, 1506, 1429, 1384, 1282, 1146, 1067, 913, 847, 807, 759, 705, 686, 634, 612, 535, 488, 437, 412 cm^{-1}.

*N^4-Benzyl-3,5-bis-chloromethyl-1,2,4-triazole Hydrochloride (**3f**).* The reaction of **2f** (0.50 g, 2.3 mmol) and 10 mL of $SOCl_2$ according to the general procedure gave the desired product as pale yellow crystalline solid (0.59 g, 87%). Anal. Calcd for $C_{11}H_{12}N_3Cl_3$ (292.59 g mol^{-1}): C 45.15, H 4.13, N 14.36. Found: C 45.39, H 4.38, N 14.34%. δ_H (500 MHz, d_6-DMSO): 4.87 (s, 4H, H^1), 5.44 (s, 2H, H^3), 7.18 (d, 2H, 6 Hz, H^5), 7.33−7.41 (m, 3H H^6 and H^7). δ_C (125 MHz, d_6-DMSO): 33.8 (C^1), 46.9 (C^3), 126.9 (C^5), 128.2 (C^7), 128.9 (C^6), 134.6 (C^4), 152.4 (C^2). IR (KBr): 3407, 2928, 2202, 1858, 1588, 1497, 1447, 1425, 1343, 1317, 1293, 1271, 1235, 1221, 1157, 1102, 1041, 1026, 960, 943, 905, 804, 790, 759, 741, 725, 704, 690, 666, 470, 459 cm^{-1}.

*N^4-iso-Butyl-3,5-bis-chloromethyl-1,2,4-triazole Hydrochloride (**3g**).* The reaction of **2g** (0.50 g, 2.7 mmol) and 10 mL of $SOCl_2$ according to the general procedure gave the desired product **3g** as a colorless crystalline solid (0.54 g, 78%). Anal. Calcd for $C_8H_{14}N_3Cl_3$ (258.58 g mol^{-1}): C 37.16, H 5.46, N 16.25. Found: C 37.60, H 5.55, N 16.62%. δ_H (300 MHz, d_6-DMSO): 0.88 (d, 6H, 7 Hz, H^5), 2.19 (m, 1H, H^4), 3.95 (d, 2H, 8 Hz, H^3), 5.00 (s, 4H, H^1). δ_C (75 MHz, d_6-DMSO): 19.2 (C^5), 28.1 (C^4), 33.9 (C^1), 50.3 (C^3), 152.2 (C^2). IR (KBr): 3384, 2970, 2932, 2875, 2257, 1885, 1579, 1534, 1496, 1468, 1447, 1392, 1371, 1340, 1285, 1278, 1225 1179, 1161, 1106, 1015, 976, 928, 882, 794, 757, 717, 661, 599, 478 cm^{-1}.

*N^4-Hexadecyl-3,5-bis-chloromethyl-1,2,4-triazole Hydrochloride (**3h**).* The reaction of **2h** (0.547 g, 1.6 mmol) and 10 mL of $SOCl_2$ according to the general procedure gave the desired product **3h** as a colorless crystalline solid (0.60 g, 90%). Anal. Calcd for $C_{20}H_{38}N_3Cl_3$ (426.89 g mol^{-1}): C 56.27, H 8.97, N 9.84. Found: C 56.52, H 9.24, N 9.93%. δ_H (300 MHz, d_6-DMSO): 0.86 (t, 3H, 6.6 Hz, H^{18}), 1.25 (m, br, 26H, H$^{5-17}$), 1.74 (m, 2H, 6.6 Hz, H^4), 4.03 (t, 2H, 7.8 Hz H^3), 4.99 (s, 4H, H^1). δ_C (75 MHz, d_6-DMSO): 13.9 (C^{18}), 22.1−31.3 (C$^{3-17}$), 53.3 (C^1), 155.2 (C^2). IR (KBr): 3448, 2916, 2852, 2218, 1881, 1581, 1536, 1503, 1473, 1378, 1352, 1287, 1272, 1227, 1152, 1099, 1022, 1004, 976, 896, 797, 788, 715, 662, 602, 413 cm^{-1}.

*General Procedure for Preparation of N^4-Substituted-3,5-bis-{[(2-pyridylmethyl)amino]methyl}-4H-1,2,4-triazoles (**PMRT** Ligands).* A mixture of N^4-substituted-3,5-bis-chloromethyl-1,2,4-triazole hydrochloride (1 equiv), 2-aminomethylpyridine (4 equiv), and potassium carbonate (6 equiv) was refluxed in dry acetonitrile (50 mL) for 7 h. The resulting yellow mixture was filtered through Celite to give a clear yellow solution. Removal of the solvent in vacuo gave pale orange/brown oil which contained the desired product and 2-aminomethylpyridine starting material. Purification was achieved by dissolving the crude oil in methanol/ethanol (1:5) and filtering it through a short pad of neutral alumina. Removal of the solvent gave **PMRT** as an orange oil with a small amount of 2-aminomethylpyridine. These oils could be used for complexation reactions without further purification. Any deviation from this procedure is detailed below.

*N^4-Pyrrolyl-3,5-bis{[(2-pyridylmethyl)amino]methyl}-4H-1,2,4-triazole (**PMPT**).* With 924 mg of N^4-pyrrolyl-3,5-bis(chloromethyl)-1,2,4-triazole (4.00 mmol) to start with and the general procedure, the desired product **PMPT** was obtained as an orange oil (1.3 g). δ_H (300 MHz, $CDCl_3$): 3.77 (s, 4H, H^6), 3.90 (s, 4H, H^7), 6.32 (t, 2H, 2.2 Hz, H^{10}), 6.88 (t, 2H, 2.2 Hz, H^9), 7.14 (dd, 2H, 7.8, 4.8 Hz, H^2), 7.22 (d, 2H, 7.8 Hz, H^4), 7.61 (td, 2H, 7.8, 1.1 Hz, H^3), 8.51 (dd, 2H, 4.8,1.1 Hz, H^1). ESI-MS (+): m/z = 397.1854 [(**PMPT**) + Na]$^+$(calcd = 397.1870).

*N^4-N,N-Diphenylamino-3,5-bis{[(2-pyridylmethyl)amino]methyl}-4H-1,2,4-triazole (**PM^{Ph}AT**).* This reaction started with 200 mg of N^4-N,N-diphenylamino-3,5-bis-chloromethyl-1,2,4-triazole (0.60 mmol) and followed the general procedure; however, the reaction time was extended to 24 h. The desired product **PM^{Ph}AT** was obtained as an orange/brown oil, but after filtration through alumina, there was still heavy contamination by unreacted N^4-N,N-diphenylamino-3,5-bis-chloromethyl-1,2,4-triazole (150 mg). The higher contamination in this system did not affect the complexation with iron(II), and the orange/brown oil was used without further purification. δ_H (300 MHz, $CDCl_3$): 3.74 (s, 4H, H^7), 3.79 (s, 4H, H^6), 6.96−7.34

dx.doi.org/10.1021/ic4014416 | Inorg. Chem. 2013, 52, 11185−11199

(m, 14H, H^{10-12}, H^2, and H^4), 7.55 (td, 2H, 7.6, 1.8 Hz, H^3), 8.48 (dd, 2H, 4.9, 0.8 Hz, H^1). ESI-MS (+): m/z = 477.261 [(**PM^{Ph}AT**) + H]$^+$ (calcd = 477.251).

N^4-Phenyl-3,5-bis{[(2-pyridylmethyl)amino]methyl}-4H-1,2,4-triazole (PMPhT). With 100 mg of N^4-phenyl-3,5-bis-chloromethyl-1,2,4-triazole hydrochloride (0.31 mmol) to start and the general procedure, the desired product **PMPhT** was obtained as an orange oil (70 mg, 58%). δ_H (300 MHz, $CDCl_3$: 3.81 (s, 4H, H^7), 3.91 (s, 4H, H^6), 7.11 (t, 2H, 7 Hz, H^2), 7.20 (d, 2H, 7.8 Hz, H^4), 7.37 (m, 3H, H^{10} and H^{12}), 7.48 (m, 2H, 4.5 Hz, H^{11}), 7.57 (t, 2H, 3.9 Hz, H^3), 8.44 (d, 2H, 4.2 Hz, H^1). ESI-MS (+): m/z = 386.211 [(**PMPhT**) + H]$^+$ (calcd = 386.209).

N^4-(3,5-Bis-trifluoromethylphenyl)-3,5-bis{[(2-pyridylmethyl)-amino]methyl}-4H-1,2,4-triazole (PM^{CF3}PhT). With 200 mg of N^4-3,5-bis-trifluoromethylphenyl-3,5-bis-chloromethyl-1,2,4-triazole (0.54 mmol) to start and the general procedure, the desired product **PM^{CF3}PhT** was obtained as an orange oil (210 mg). δ_H (300 MHz, $CDCl_3$): 3.71 (s, 4H, H^7), 3.79 (s, 4H, H^6), 7.21−7.06 (m, 4H, $H^{2,4}$), 7.53 (td, 2H, 7.7, 1.7 Hz, H^3), 7.93 (s, 1H, H^{12}), 8.19 (s, 2H, H^{10}), 8.43 (ddd, 2H, 4.8, 1.7, 1.1 Hz, H^1). ESI-MS (+): m/z = 522.185 [(**PM^{CF3}PhT**) + H]$^+$ (calcd = 522.176).

N^4-Benzyl-3,5-bis{[(2-pyridylmethyl)amino]methyl}-4H-1,2,4-triazole (PMBzT). With 300 mg of N^4-benzyl-3,5-bis-chloromethyl-1,2,4-triazole hydrochloride (1.03 mmol) to start and the general procedure, the desired product **PMBzT** was obtained as an orange oil (350 mg). δ_H (300 MHz, d_6-DMSO): 3.75 (s, 8H, H^6 and H^7), 5.44 (s, 2H, H^9), 7.07 (dd, 2H, 7.7, 1.7 Hz, H^4), 7.33−7.19 (m, 5H, H^{11-13} and H^2), 7.70 (td, 2H, 7.6, 1.8 Hz, H^3), 8.47 (ddd, 2H, 4.8, 1.8, 0.9 Hz, H^1). ESI-MS (+): m/z = 400.226 [(**PMBzT**) + H]$^+$ (calcd = 400.224).

N^4-iso-Butyl-3,5-bis{[(2-pyridylmethyl)amino]methyl}-4H-1,2,4-triazole (PMibT). With 260 mg of N^4-isobutyl-3,5-bis-chloromethyl-1,2,4-triazole hydrochloride (1.01 mmol) to start and the general procedure, the desired product **PMibT** was obtained as an orange oil (254 mg). δ_H (300 MHz, d_6-DMSO): 0.82 (d, 6H, 6.7 Hz, H^{11}), 2.02 (m, 1H, H^{10}), 3.88−3.94 (m, 6H, H^6, H^7, and H^9), 7.13 (m, 2H, H^4), 7.27 (dd, 2H, 8.3, 5.0 Hz, H^2), 7.62 (td, 2H, 7.7, 1.7 Hz, H^3), 8.53 (d, 2H, 4 Hz, H^1). ESI-MS (+): m/z = 366.240 [(**PMibT**) + H]$^+$ (calcd = 366.240).

N^4-Hexadecyl-3,5-bis{[(2-pyridylmethyl)amino]methyl}-4H-1,2,4-triazole (PMC$_{16}$T). With 157 mg of N^4-hexadecyl-3,5-bis-chloromethyl-1,2,4-triazole hydrochloride (0.37 mmol) to start and the general procedure, the desired product **PMC$_{16}$T** was obtained as an orange oil (112 mg). δ_H (300 MHz, $CDCl_3$): 0.89 (t, 3H, 6.7 Hz, H^{24}), 1.26 (m, br, 26H, H^{11-23}), 1.69 (m, 2H, H^{10}) 3.95 (s, 4H, H^7), 3.98 (s, 4H, H^6), 4.07 (t, 2H, 6.7 Hz, H^9), 7.18 (dd, 2H, 6.5, 5.0 Hz, H^4), 7.30 (d, 2H, 7.8 Hz, H^2), 7.65 (ddd, 2H, 7.7, 6.0, 1.8 Hz, H^3), 8.56 (d, 2H, 4.2 Hz, H^1). ESI-MS (+): m/z = 534.428 [(**PMC$_{16}$T**) + H]$^+$ (calcd = 534.428).

Synthesis of Complexes. *[Fe$^{II}_2$(PMPT)$_2$](BF$_4$)$_4$.* To a clear, pale yellow solution of **PMPT** (37 mg, 0.10 mmol) in methanol (5 mL) was added a colorless solution of iron(II) tetrafluoroborate hexahydrate (34 mg, 0.10 mmol) in methanol (2.5 mL), causing the immediate formation of a very pale yellow precipitate. The reaction was stirred at room temperature, open to the air for 30 min, and then capped and left to stand overnight. The solid was then isolated by filtration, washed with methanol (5 mL), and dried thoroughly in vacuo. Yield: 33 mg (55%). Anal. Calcd for $[Fe_2(C_{20}H_{22}N_8)_2](BF_4)_4\cdot H_2O$ (1225.82 g mol^{-1}): C 39.78, H 3.67, N 18.56. Found: C 39.66, H 3.83, N 18.47%. ESI-MS (+): m/z = 1121.259 [Fe$^{II}_2$(**PMPT**)$_2$](BF$_4$)$_3$]$^+$ (calcd = 1121.273). IR (ATR): 3329, 1610, 1559, 1444, 1277, 1051, 925, 897, 775, 732, 522 cm^{-1}.

[Fe$^{II}_2$(PM^{Ph}AT)$_2$](BF$_4$)$_4$. To a stirred orange solution of **PM^{Ph}AT** (140 mg, 0.3 mmol) in methanol (10 mL) was added, dropwise with stirring at room temperature, a solution of iron(II) tetrafluoroborate hexahydrate (197 mg, 0.6 mmol) in methanol (5 mL). On addition a voluminous pale precipitate formed, and the mixture was left to stir for 1 h before the precipitate was filtered. Filtration and drying in vacuo yielded an off-white solid (85 mg, 40%). Anal. Calcd for $[Fe_2(C_{28}H_{28}N_8)_2](BF_4)_4$ (1412.08 g mol^{-1}): C 47.63, H 4.00, N 15.87. Found: C 47.57, H 4.15, N 15.74%. Recrystallization from MeCN/DMF (4:1) gave a pale off-white crystalline solid. Anal. Calcd for $[Fe_2(C_{28}H_{28}N_8)_2](BF_4)_4$ (1412.08 g mol^{-1}): C 47.63, H 4.00, N 15.87. Found: C 47.71, H 4.26, N 15.97%. ESI-MS (+): m/z = 1325.359 [Fe$^{II}_2$(**PM^{Ph}AT**)$_2$](BF$_4$)$_3$]$^+$ (calcd = 1325.368). IR (ATR): 3324, 3067, 1608, 1552, 1489, 1443, 1287, 1049, 902, 775, 760, 694, 519 cm^{-1}.

[Fe$^{II}_2$(PMPhT)$_2$](BF$_4$)$_4$. To a stirred orange solution of **PMPhT** (113 mg, 0.29 mmol) in methanol (20 mL) was added, dropwise with stirring at room temperature, a methanolic solution (5 mL) of iron(II) tetrafluoroborate hexahydrate (147 mg, 0.44 mmol). On addition, a voluminous pale precipitate formed, and the mixture was left to stir for 1 h before the precipitate was filtered. Filtration and drying in vacuo yielded an off-white solid (138 mg, 39%). Anal. Calcd for $[Fe_2(C_{22}H_{23}N_7)_2](BF_4)_4\cdot H_2O$ (1247.87 g mol^{-1}): C 42.35, H 3.88, N 15.71. Found: C 42.27, H 3.82, N 15.49%. Recrystallization from MeCN/DMF (4:1) gave purple crystalline solid. Anal. Calcd for $[Fe_2(C_{22}H_{23}N_7)_2](BF_4)_4$ (1229.85 g mol^{-1}): C 42.97, H 3.77, N 15.94. Found: C 43.01, H 3.84, N 15.94%. ESI-MS (+): m/z = 1143.272 [Fe$^{II}_2$(**PMPhT**)$_2$](BF$_4$)$_3$]$^+$ (calcd = 1143.283). IR (ATR): 3326, 1609, 1552, 1503, 1444, 1309, 1049, 899, 771, 699, 521 cm^{-1}.

[Fe$^{II}_2$(PM^{CF3}PhT)$_2$](BF$_4$)$_4$. To a stirred orange solution of **PM^{CF3}PhT** (150 mg, 0.28 mmol) in methanol (10 mL) was added, dropwise with stirring at room temperature, a methanolic solution (5 mL) of iron(II) tetrafluoroborate hexahydrate (144 mg, 0.43 mmol). On addition a voluminous pale precipitate formed, and the mixture was left to stir for 1 h before the precipitate was filtered. Filtration and drying in vacuo yielded an off-white solid (109 mg, 51%). Anal. Calcd for $[Fe_2(C_{24}H_{21}N_7F_6)_2](BF_4)_4\cdot H_2O$ (1519.86 g mol^{-1}): C 37.93, H 2.92, N 12.90, F 35.00. Found: C 38.12, H 3.04, N 13.11, F 34.71%. Recrystallization from MeCN/DMF (4:1) gave a pale off-white powder. $Fe_2(C_{24}H_{21}N_7F_6)_2](BF_4)_4\cdot DMF\cdot H_2O$ (1592.95 g mol^{-1}): C 38.45, H 3.23, N 13.19, F 33.39. Found: C 38.36, H 3.45, N 12.96, F 33.11%. ESI-MS (+): m/z = 1415.228 [Fe$^{II}_2$(**PM^{CF3}PhT**)$_2$](BF$_4$)$_3$]$^+$ (calcd = 1415.233). IR (ATR): 3556, 3328, 1610, 1547, 1444, 1318, 1047, 898, 770, 706, 522 cm^{-1}.

Fe$^{II}_2$(PMBzT)$_2$](BF$_4$)$_4$. To a stirred orange solution of **PMBzT** (200 mg, 0.5 mmol) in methanol (20 mL) was added, dropwise with stirring at room temperature, a solution of iron(II) tetrafluoroborate hexahydrate (335 mg, 1 mmol) in methanol (5 mL). On addition a pale precipitate formed, and the mixture was left to stir for 1 h before the precipitate was filtered. Filtration and drying in vacuo yielded an off-white solid (146 mg, 46%).Anal. Calcd for $[Fe_2(C_{23}H_{26}N_7)_2](BF_4)_4\cdot 2H_2O$ (1295.95 g mol^{-1}): C 42.63, H 4.36, N 15.13. Found: C 42.42, H 4.22, N 15.02%. Recrystallization from MeCN/DMF (4:1) gave a pale off-white crystalline solid. Anal. Calcd for $[Fe_2(C_{23}H_{26}N_7)_2](BF_4)_4$ (1259.92 g mol^{-1}): C 43.85, H 4.16, N 15.56. Found: C 43.80, H 4.15, N 15.85%. ESI-MS (+): m/z = 1171.308 [Fe$^{II}_2$(**PMBzT**)$_2$](BF$_4$)$_3$]$^+$ (calcd = 1171.315). IR (ATR): 3554, 3327, 1646, 1608, 1549, 1444, 1309, 1019, 897, 772, 710, 520 cm^{-1}.

[Fe$^{II}_2$(PMibT)$_2$](BF$_4$)$_4$. To a stirred orange solution of **PMibT** (200 mg, 0.66 mmol) in methanol (20 mL) was added, dropwise with sitrring at room temperature, a methanolic solution (5 mL) of iron(II) tetrafluoroborate hexahydrate (442 mg, 1.19 mmol). On addition a pale precipitate formed, and the mixture was left to stir for 1 h before the precipitate was filtered. Filtration under argon and drying in vacuo yielded an off-white solid (135 mg, 32%). Anal. Calcd for $[Fe_2(C_{20}H_{27}N_7)_2](BF_4)_4\cdot 4H_2O$ (1261.93 g mol^{-1}): C 38.07, H 4.95, N 15.54. Found: C 38.18, H 4.55, N 15.49%. Recrystallization from MeCN/DMF (4:1) gave a very pale purple powder. Anal. Calcd for $[Fe_2(C_{20}H_{20}N_7)_2](BF_4)_4\cdot 3H_2O$ (1175.76 g mol^{-1}): C 38.62, H 4.86, N 15.76. Found: C 38.78, H 4.49, N 15.77%. ESI-MS (+): m/z = 1103.341 [Fe$^{II}_2$(**PMibT**)$_2$](BF$_4$)$_3$]$^+$ (calcd = 1103.330). IR (ATR): 3329, 2965, 1611, 1553, 1443, 1312, 1049, 897, 771, 724, 523 cm^{-1}.

[Fe$^{II}_2$(PMC$_{16}$T)$_2$](BF$_4$)$_4$. To a stirred orange solution of **PMC$_{16}$T** (30 mg, 0.05 mmol) in methanol (5 mL) was added, dropwise with stirring at room temperature, a methanolic solution (2.5 mL) of iron(II) tetrafluoroborate hexahydrate (28 mg, 0.084 mmol). On addition a pale precipitate formed, and the mixture was left to stir for 1 h before the precipitate was filtered. Filtration under argon and drying in vacuo yielded an off-white solid (25 mg, 33%). Anal. Calcd for $[Fe_2(C_{32}H_{51}N_7)_2](BF_4)_4$ (1526.52 g mol^{-1}): C 50.36, H 6.73, N 12.85.

Found: C 50.16, H 6.86, N 12.78%. ESI-MS (+): m/z = 1439.724 $[Fe^{II}_2(\mathbf{PMC_{16}T})_2](BF_4)_3]^+$ (calcd = 1439.722). IR (ATR): 3326, 2922, 2852, 1609, 1549, 1490, 1444, 1312, 1020, 900, 772, 722, 520 cm^{-1}.

■ ASSOCIATED CONTENT

Supporting Information

X-ray crystallography information for the complexes and 3,5-bis-dichloromethyl-N^4-substituted triazoles (CCDC 921920, 921921, 921923−921927) as well as magnetochemistry and Mössbauer spectroscopy details. Crystallographic data in CIF format. This material is available free of charge via the Internet at http://pubs.acs.org.

■ AUTHOR INFORMATION

Corresponding Author

*E-mail: sbrooker@chemistry.otago.ac.nz. Phone: +64 3 4797919. Fax: +64 3 4797906.

Notes

The authors declare no competing financial interest.

■ ACKNOWLEDGMENTS

This work was supported by grants from the University of Otago, the MacDiarmid Institute for Advanced Materials and Nanotechnology, and the RSNZ Marsden Fund.

■ REFERENCES

(1) (a) Kahn, O.; Codjovi, E. *Phil. Trans. R. Soc., A* **1996**, *354*, 359−379. (b) Haasnoot, J. G. *1,2,4-Triazoles as Ligands for Iron(II) High Spin-Low Spin Crossovers*; Kluwer Academic Publishers: Dordrecht, 1996; pp 299−321. (c) Kahn, O. *Chem. Br.* **1999**, *2*, 24−27. (d) Létard, J.-F.; Guionneau, P.; Goux-Capes, L. *Top. Curr. Chem.* **2004**, *234*, 221−250. (e) Gaspar, A. B.; Muñoz, M. C.; Real, J. A. *J. Mater. Chem.* **2006**, 2522−2533. (f) Brooker, S.; Kitchen, J. A. *Dalton Trans.* **2009**, 7331−7340 and front cover image. (g) Wang, Y.-T.; Li, S.-T.; Wu, S.-Q.; Cui, A.-L.; Shen, D.-Z.; Kou, H.-Z. *J. Am. Chem. Soc.* **2013**, *135*, 5938−5941.

(2) (a) Breuning, E.; Ruben, M.; Lehn, J.-M.; Renz, F.; Garcia, Y.; Ksenofontov, V.; Gütlich, P.; Wegelius, E.; Rissanen, K. *Angew. Chem., Int. Ed.* **2000**, *39*, 2504−2507. (b) Ruben, M.; Breuning, E.; Lehn, J.-M.; Ksenofontov, V.; Renz, F.; Gütlich, P.; Vaughan, G. B. M. *Chem.—Eur. J.* **2003**, *9*, 4422−4429. (c) Schneider, B.; Demeshko, S.; Dechert, S.; Meyer, F. *Angew. Chem., Int. Ed.* **2010**, *49*, 9274−9277. (d) Wei, R.-J.; Huo, Q.; Tao, J.; Huang, R.-B.; Zheng, L.-S. *Angew. Chem., Int. Ed.* **2011**, *50*, 8940−8943. (e) Ferguson, A.; Squire, M. A.; Siretanu, D.; Mitcov, D.; Mathonière, C.; Clérac, R.; Kruger, P. E. *Chem. Commun.* **2013**, *49*, 1597−1599. (f) Bilbeisi, R. A.; Zarra, S.; Feltham, H. L. C.; Jameson, G. N. L.; Clegg, J. K.; Brooker, S.; Nitschke, J. R. *Chem.—Eur. J.* **2013**, *19*, 8058−8062.

(3) Olguín, J.; Brooker, S. Spin crossover in discrete polynuclear complexes. In *Spin-Crossover Materials: Properties and Applications*, 1st ed.; Halcrow, M. A., Ed.; John Wiley & Sons, Ltd: New York, 2013; pp 77−120.

(4) Nakano, K.; Suemura, N.; Yoneda, K.; Kawata, S.; Kaizaki, S. *Dalton Trans.* **2005**, 740−743.

(5) (a) Kunkeler, P. J.; van Koningsbruggen, P. J.; Cornelissen, J. P.; van der Horst, A. N.; van der Kraan, A. M.; Spek, A. L.; Haasnoot, J. G.; Reedijk, J. *J. Am. Chem. Soc.* **1996**, *118*, 2190−2197. (b) Moliner, N.; Muñoz, M. C.; van Koningsbruggen, P. J.; Real, J. A. *Inorg. Chim. Acta* **1998**, *274*, 1−6. (c) Moliner, N.; Gaspar, A. B.; Muñoz, M. C.; Niel, V.; Cano, J.; Real, J. A. *Inorg. Chem.* **2001**, *40*, 3986−3991. (d) Zhu, D.; Xu, Y.; Yu, Z.; Guo, Z.; Sang, H.; Liu, T.; You, X. *Chem. Mater.* **2002**, *14*, 838−843. (e) Kitchen, J. A.; Brooker, S. *Coord. Chem. Rev.* **2008**, *252*, 2072−2092. (f) Dupouy, G.; Marchivie, M.; Triki, S.; Sala-Pala, J.; Salaün, J.-Y.; Gómez-García, C. J.; Guionneau, P. *Inorg. Chem.* **2008**, *47*, 8921−8931. (g) Kitchen, J. A.; Jameson, G. N. L.; Tallon, J. L.; Brooker, S. *Chem. Commun.* **2010**, *46*, 3200−3202.

(6) Moliner, N.; Muñoz, M. C.; Létard, S.; Létard, J.-F.; Solans, X.; Burriel, R.; Castro, M.; Kahn, O.; Real, J. A. *Inorg. Chim. Acta* **1999**, *291*, 279−288.

(7) Gaspar, A. B.; Muñoz, M. C.; Moliner, N.; Ksenofontov, V.; Levchenko, G.; Gütlich, P.; Real, J. A. *Monatsh. Chem.* **2003**, *134*, 285−294.

(8) (a) Klingele, M. H.; Brooker, S. *Coord. Chem. Rev.* **2003**, *241*, 119−132. (b) Klingele, M. H.; Brooker, S. *Eur. J. Org. Chem.* **2004**, 3422−3434. (c) Klingele, J.; Scherer, H.; Klingele, M. H. *Z. Anorg. Allg. Chem.* **2009**, *635*, 2279−2287.

(9) Kitchen, J. A.; Noble, A.; Brandt, C. D.; Moubaraki, B.; Murray, K. S.; Brooker, S. *Inorg. Chem.* **2008**, *47*, 9450−9458.

(10) Kitchen, J. A.; White, N. G.; Boyd, M.; Moubaraki, B.; Murray, K. S.; Boyd, P. D. W.; Brooker, S. *Inorg. Chem.* **2009**, *48*, 6670−6679.

(11) Kitchen, J. A.; White, N. G.; Gandolfi, C.; Albrecht, M.; Jameson, G. N. L.; Tallon, J. L.; Brooker, S. *Chem. Commun.* **2010**, *46*, 6464−6466.

(12) Miller, R. G.; Jameson, G. N. L.; Olguín, J.; Brooker, S. *Supramol. Chem.* **2012**, *24*, 547−552.

(13) Shen, G.-P.; Qi, L.; Wang, L.; Xu, Y.; Jiang, J.-J.; Zhu, D.; Liu, X.-Q.; You, X. *Dalton Trans.* **2013**, *42*, 10144−10152.

(14) Klingele, M. H.; Moubaraki, B.; Murray, K. S.; Brooker, S. *Chem.—Eur. J.* **2005**, *11*, 6962−6973.

(15) Klingele, M. H.; Moubaraki, B.; Cashion, J. D.; Murray, K. S.; Brooker, S. *Chem. Commun.* **2005**, 987−989.

(16) (a) Grunert, C. M.; Reiman, S.; Spiering, H.; Kitchen, J. A.; Brooker, S.; Gütlich, P. *Angew. Chem., Int. Ed.* **2008**, *47*, 2997−2999. (b) Bhattacharjee, A.; Ksenofontov, V.; Kitchen, J. A.; White, N. G.; Brooker, S.; Gütlich, P. *Appl. Phys. Lett.* **2008**, *92*, 174104. (c) Bhattacharjee, A.; Roy, M.; Ksenofontov, V.; Kitchen, J. A.; Brooker, S.; Gütlich, P. *Eur. J. Inorg. Chem.* **2013**, 843−849.

(17) Bartlett, R. K.; Humphrey, I. R. *J. Chem. Soc.* **1967**, *C*, 1664−1666.

(18) (a) Samano, V.; Miles, R. W.; Robins, M. J. *J. Am. Chem. Soc.* **1994**, *116*, 9331−9332. (b) Miles, R. W.; Samano, V.; Robins, M. J. *J. Am. Chem. Soc.* **1995**, *117*, 5951−5957. (c) Robins, M. J.; Miles, R. W.; Samano, M. C.; Kaspar, R. L. *J. Org. Chem.* **2001**, *66*, 8204−8210.

(19) (a) Seidel, M. C.; Von Meyer, W. C.; Greenfield, S. A. 1,2,4-4*H*-Triazole Derivatives. 4,120,864, 1978. (b) Díez-Barra, E.; de la Hoz, A.; Rodríguez-Curiel, R. I.; Tejeda, J. *Tetrahedron* **1997**, *53*, 2253−2260. (c) Alcarazo, M.; Fernández, R.; Álvarez, E.; Lassaletta, J. M. *J. Organomet. Chem.* **2005**, *690*, 5979−5988. (d) Naik, A. D.; Marchand-Brynaert, J.; Garcia, Y. *Synthesis* **2008**, 149−154.

(20) Hester, J. B. *J. Heterocycl. Chem.* **1980**, *17*, 575−581.

(21) (a) Ivanova, N. V.; Sviridov, S. I.; Shorshnev, S. V.; Stepanov, A. E. *Synthesis* **2006**, 156−160. (b) Ivanova, N. V.; Sviridov, S. I.; Stepanova, A. E. *Tetrahedron Lett.* **2006**, *47*, 8025−8027.

(22) White, N. G.; Feltham, H. L. C.; Gandolfi, C.; Albrecht, M.; Brooker, S. *Dalton Trans.* **2010**, *39*, 3751−3758.

(23) Talham, D. R. *Chem. Rev.* **2004**, *104*, 5479−5501.

(24) Weber, B. *Coord. Chem. Rev.* **2009**, *253*, 2432−2449.

(25) (a) Klingele, M. H.; Boyd, P. D. W.; Moubaraki, B.; Murray, K. S.; Brooker, S. *Eur. J. Inorg. Chem.* **2006**, 573−589. (b) Hellyer, R. M.; Joule, J. A.; Larsen, D. S.; Brooker, S. *Acta Crystallogr., Sect. C* **2007**, *C63*, o358−o360.

(26) White, N. G.; Kitchen, J. A.; Brooker, S. *Eur. J. Inorg. Chem.* **2009**, 1172−1180.

(27) Desiraju, G. R.; Steiner, T. *The Weak Hydrogen Bond in Structural Chemistry and Biology*; Oxford University Press: Oxford, 1999.

(28) (a) Gamez, P.; Mooibroek, T. J.; Teat, S. J.; Reedijk, J. *Acc. Chem. Res.* **2007**, *40*, 435−444. (b) Schottel, B. L.; Chifotides, H. T.; Dunbar, K. R. *Chem. Soc. Rev.* **2008**, *37*, 68−83. (c) Salonen, L. M.; Ellermann, M.; Diederich, F. *Angew. Chem., Int. Ed.* **2011**, *50*, 4808−4842. (d) Frontera, A. *Coord. Chem. Rev.* **2013**, *257*, 1716−1727.

(29) Brooker, S.; White, N. G.; Bauzá, A.; Deyà, P. M.; Frontera, A. *Inorg. Chem.* **2012**, *51*, 10334−10340.

(30) van der Sluis, P.; Spek, A. L. *Acta Crystallogr., Sect. A* **1990**, *A46*, 194−201.

(31) Thompson, L. K.; Waldmann, O.; Xu, Z., *Coord. Chem. Rev.* **2005**, *249*, 2677-2690. MAGMUN4.11/OW01.exe is available as a combined package free of charge from the authors (http://www.ucs.mun.ca/~lthomp/magmun). MAGMUN was developed by Dr. Zhiqiang Xu (Memorial University), and OW01.exe by Dr O.Waldmann.
(32) Olguín, J.; Jameson, G. N. L.; Brooker, S. *Dalton Trans.* **2011**, *40*, 5086−5089.
(33) Kitchen, J. A.; White, N. G.; Jameson, G. N. L.; Tallon, J. L.; Brooker, S. *Inorg. Chem.* **2011**, *50*, 4586−4597.
(34) (a) Greenwood, N. N.; Gibb, T. C., *Mössbauer Spectroscopy*; Chapman and Hall Ltd: London, 1971; p 659. (b) Gütlich, P.; Bill, E.; Trautwein, A. X., *Mössbauer Spectroscopy and Transition Metal Chemistry*; Springer-Verlag: Berlin, 2011.
(35) Psomas, G.; Bréfuel, N.; Dahan, F.; Tuchagues, J.-P. *Inorg. Chem.* **2004**, *43*, 4590−4594.
(36) The only complex for which magnetic data are not consistent with the Mössbauer data is $[Fe^{II}_2(\mathbf{PM^{CF3}PhT})_2](BF_4)_4{\cdot}DMF{\cdot}H_2O$ (Table 4). However, this sample was measured again one month later, and the %HS had decreased (Supporting Information Figure S26). These changes over time are probably due to small changes in solvation, which may well explain the discrepancies between the magnetic and Mössbauer data, as the Mössbauer spectra were recorded on these samples up to four weeks after the magnetic data were collected.
(37) Jameson, G. N. L.; Werner, F.; Bartel, M.; Absmeier, A.; Reissner, M.; Kitchen, J. A.; Brooker, S.; Caneschi, A.; Carbonera, C.; Létard, J.-F.; Linert, W. *Eur. J. Inorg. Chem.* **2009**, *26*, 3948−3959.
(38) Gottlieb, H. E.; Kotlyar, V.; Nudelman, A. *J. Org. Chem.* **1997**, *62*, 7512−7515.
(39) Sheldrick, G. M. *SADABS. Empirical Absorption Correction Program for Area Detector Data*; University of Göttingen: Göttingen, 1996.
(40) Sheldrick, G. M. *Acta Crystallogr., Sect. A* **2008**, *A64*, 112−122.
(41) Macrae, C. F.; Bruno, I. J.; Chisholm, J. A.; Edgington, P. R.; McCabe, P.; Pidcock, E.; Rodriguez-Monge, L.; Taylor, R.; van de Streek, J.; Wood, P. A. *J. Appl. Crystallogr.* **2008**, *41* (2), 466−470.
(42) *Persistence of Vision Raytracer (Version 3.6)*; POVray Persistence of Vision Pty. Ltd. Williamstown, Australia, 2004.

■ NOTE ADDED AFTER ASAP PUBLICATION

Due to a production error, this paper was published on the Web on September 20, 2013, with an error in the Title. The corrected version was reposted on October 7, 2013.